

ANALYSIS OF A  
REINFORCED CONCRETE BEAM IN TORSION

by  
William Aurdand Stuart II

Thesis submitted to the Graduate Faculty of the  
Virginia Polytechnic Institute  
in candidacy for the degree of  
Master of Science  
in  
Civil Engineering

March 20, 1964  
Blacksburg, Virginia

## TABLE OF CONTENTS

	PAGE
LIST OF FIGURES AND TABLES	3
ACKNOWLEDGEMENTS	6
Chapter	
I. INTRODUCTION	7
II. REVIEW OF LITERATURE	13
III. EXPERIMENTAL WORK AND RESULTS	
A. EXPERIMENTAL WORK	25
B. RESULTS	31
IV. DISCUSSION	72
V. CONCLUSIONS	81
BIBLIOGRAPHY	83
VITA	85

## LIST OF FIGURES AND TABLES

FIGURE	TITLE	PAGE
1-1	Examples of Combined Bending and Torsion	9
1-2	Failure Surface -- Pure Torsion	11
2-1	Example of Gesund's Dowel Action	20
3-1	Photograph of Beams Curing in the Forms	28
3-2	Photograph of Strain Gage Before Waxing	29
3-3	Photograph of Strain Gage After Waxing	29
3-4	Photograph of General Testing Arrangement	30
3-5	Strain Gage Locations, Beam 1-1	35
3-6	Strain Gage Locations, Beam 1-2	36
3-7	Strain Gage Locations, Beam 1-3	37
3-8	Strain Gage Locations, Beam 1-4	38
3-9	Strain Gage Locations, Beam 2-1	39
3-10	Strain Gage Locations, Beam 2-2	40
3-11	Strain Gage Locations, Beam 2-3	41
3-12	Strain Gage Locations, Beam 2-4	42
3-13	Torque-Strain Plot, Beam 1-1	43
3-14	Torque-Strain Plot, Beam 1-1	44
3-15	Torque-Strain Plot, Beam 1-2	45
3-16	Torque-Strain Plot, Beam 1-2	46
3-17	Torque-Strain Plot, Beam 1-3	47
3-18	Torque-Strain Plot, Beam 1-4	48
3-19	Torque-Strain Plot, Beam 2-1	49

FIGURE	TITLE	PAGE
3-20	Torque-Strain Plot, Beam 2-1	50
3-21	Torque-Strain Plot, Beam 2-2	51
3-22	Torque-Strain Plot, Beam 2-2	52
3-23	Torque-Strain Plot, Beam 2-3	53
3-24	Torque-Strain Plot, Beam 2-4	54
3-25	Angle of Principal Tensile Strain versus Torque, Beams 1-1 and 1-2	55
3-26	Angle of Principal Tensile Strain versus Torque, Beams 1-3 and 1-4	56
3-27	Angle of Principal Tensile Strain versus Torque, Beams 2-1 and 2-2	57
3-28	Angle of Principal Tensile Strain versus Torque, Beams 2-3 and 2-4	58
3-29	Angular Displacement versus Torque	59
3-30	Failure Cracks, Beam 1-1	60
3-31	Failure Cracks, Beam 1-2	61
3-32	Failure Cracks, Beam 1-3	62
3-33	Failure Cracks, Beam 1-4	63
3-34	Failure Cracks, Beam 2-1	64
3-35	Failure Cracks, Beam 2-2	65
3-36	Failure Cracks, Beam 2-3	66
3-37	Failure Cracks, Beam 2-4	67
3-38	Photograph of Failure Cracks, Beam 1-1	68
3-39	Photograph of Failure Cracks, Beam 1-1	68
3-40	Photograph of Failure Cracks, Beam 1-3	69
3-41	Photograph of Failure Cracks, Beam 1-4	69

FIGURE	TITLE	PAGE
3-42	Photograph of Failure Cracks, Beam 2-2	70
3-43	Photograph of Failure Cracks, Beam 2-2	70
3-44	Photograph of Failure Cracks, Beam 2-4	71
3-45	Photograph of Failure Cracks, Beam 2-4	71

TABLE	TITLE	PAGE
1	Properties of Test Beams	24
2	Comparison of Various Theoretical Predictions with Test Results	77

## ACKNOWLEDGEMENTS

The author would like to express his appreciation to Professor  
of the Civil Engineering Department of Virginia  
Polytechnic Institute for his leadership and guidance during the  
investigation and writing of this thesis.

Acknowledgement is also made to \_\_\_\_\_ and  
whose help in the laboratory was invaluable.

Appreciation is also expressed for the financial assistance  
given by the V. P. I. Engineering Experiment Station to purchase the  
necessary materials, without which this thesis would not have been  
possible.

Finally the author would like to express his gratitude to his  
wife for the typing and proof reading of the manuscript.

## I. INTRODUCTION

In the last forty years the use of reinforced concrete for structural purposes has increased through research and development to where it is widely used today with confidence in the most complex structures. This rapid growth can be attributed to improved cements, higher quality reinforcing steels and the advancements made in the techniques of design.

In the design of continuous structures the monolithic nature of reinforced concrete affords many advantages as well as some disadvantages. One major disadvantage is that almost every concrete member, no matter how simple, is subject to the action of combined stresses. It is often very difficult if not impossible to analyze a structure completely for every possible loading condition subjecting it to combined stresses. It is common practice in designing members to ignore any effect which produces, in the designer's opinion, negligible stresses. This may or may not always result in a safe structure. A stress which may be negligible when considered acting alone may not be negligible when combined with other stresses, and this fact may not always be evident to the designer.

In reinforced concrete members designed to resist bending the problem of torsion is usually neglected by designers in this country. However, recently this problem has been greatly emphasized in the technical literature. The subject has actually been investigated periodically since 1922, but the profession has made no recommendations

to deal with it. The Australian Code\* has a provision for dealing with torsional loads which was introduced in 1958, but its American counterpart, the American Concrete Institute Building Code,\*\* made no mention of it until 1963, and then only introduced the inference that the problem of combined bending and torsion in spandrel beams should be considered by the designer, by requiring that where stirrups are required they should be closed and provided with longitudinal corner bars.

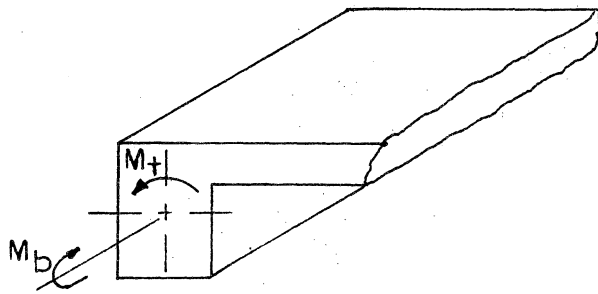
There are several good examples of structural members that are normally subjected to combined bending and torsion, where torsion is usually neglected. Perhaps the most common ones are balcony beams and girders, and building frames where a beam frames into a girder restrained by a vertical support, which causes severe torsional stresses to be developed in the girder. Spandrel beams usually experience some torsional action, and transversely loaded arches develop torsional stresses at the supports (Fig. 1-1). The torsional stress in these examples is seldom designed for, mainly because there are no known reliable methods to use, and it is assumed that the magnitude of the torsional stresses can be considered negligible.

An analytical study of the problem is extremely complex because

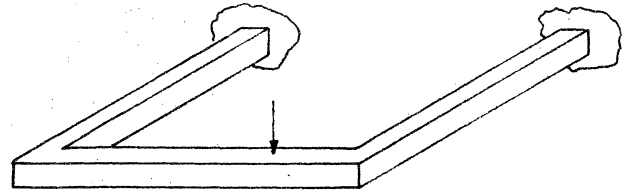
---

\*Australian Standard Rules for the Use of Normal Reinforced Concrete in Buildings, Standard Association of Australia, Sydney, 1958.

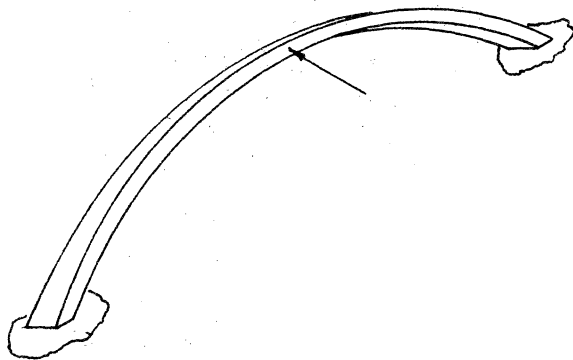
\*\*American Concrete Institute Standard Building Code Requirements for Reinforced Concrete (ACI 318 - 63), Detroit, 1963.



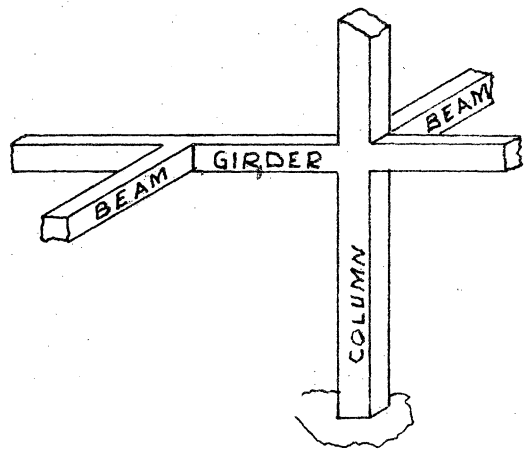
Spandrel Beam



Balcony Beam



Laterally Loaded Arch



Girder Restrained by Column

Figure 1-1 Examples of Combined Bending and Torsion

of the bi-material nature of the reinforced concrete members. Non-homogeneity of the concrete and its complex reaction to combined stresses adds further complications, not to mention the shape of the cross section.

Much work has been done along these lines, but there remain many unanswered questions to be investigated. It is the intent of this thesis to review and extend the investigation of torsional resistance of reinforced concrete beams, both experimentally and analytically. Specifically, this thesis represents a continuation of a program of study started at the University of Kentucky and Virginia Polytechnic Institute in 1959. Although the primary objective of the program is the practical analysis of torsion in combination with bending and/or shear, there is a sufficient lack of understanding of pure torsion to warrant further investigation. This thesis deals with the problem of pure torsion.

After an analytical study, eight reinforced concrete beams of square cross section, using four different spacings of stirrups, were tested in pure torsion in the laboratory. The experimental results were compared to analytical solutions using four theories of analysis. Significant differences were noted, and an attempt was made to explain the reasons for the differences. In the tests, seven of the members exhibited a very sudden brittle fracture, each with a single large crack, while the eighth developed numerous cracks and the appearance of general overall yielding.

During a test in pure torsion, as torsional loads increase, the

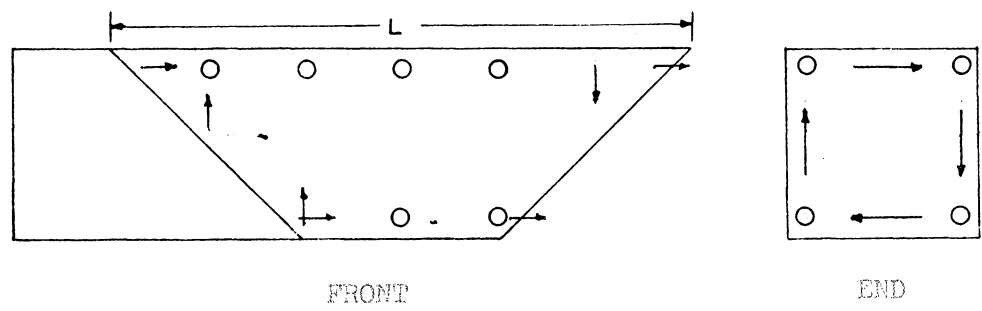
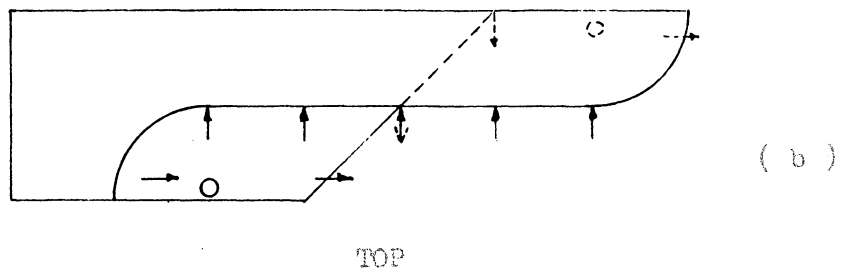
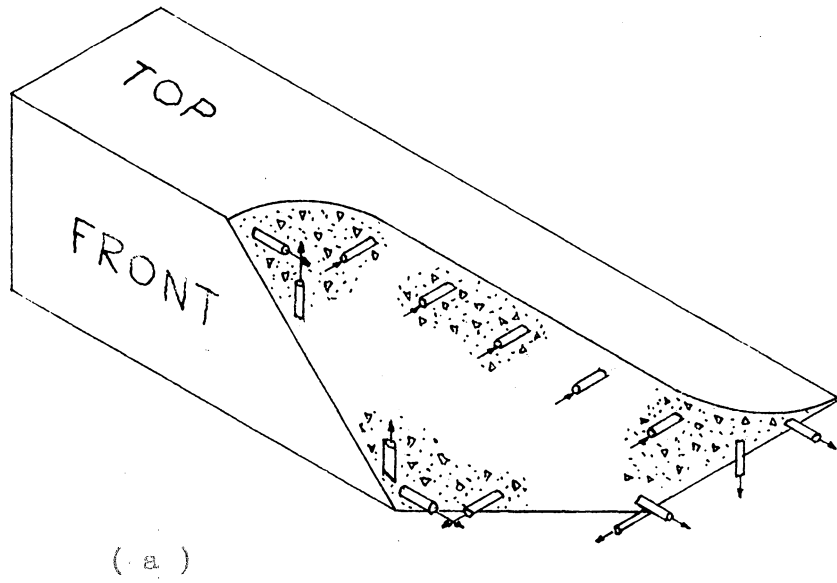


Figure 1-2 Failure Surface -- Pure Torsion

first visible indication of strain is tensile cracking of the concrete on all faces at an angle of about  $45^{\circ}$  from the longitudinal beam axis. As the load is increased further the cracks open up and a complete surface of separation is developed and defined by the connection of cracks on the several faces forming a continuous spiral. Normally one spiral crack predominates, continues around three faces and returns on itself on the fourth face, as shown in Fig. 1-2. The  $45^{\circ}$  cracks are the principal tension cracks on the three faces. The continuation on the fourth face constitutes a compression region and acts somewhat as a hinge as the ultimate load is reached.

The total length of the failure zone (L in Fig. 1-2b) is approximately three times the member's depth. It should be noted that stirrups in all faces except the face containing the hinge act in tension to resist the torque about a longitudinal axis. It should also be noted that the tension stirrups in the two faces adjacent to the face containing the hinge produce a bending moment about a transverse axis which, in turn, must be added to any bending moment induced by external forces.

Electrical resistance type strain gages were attached to the reinforcing steel and used to measure strains at selected locations. Rosette gages were used on the concrete faces of each specimen to record the concrete strains, so that principal strains and their directions could be determined.

## II. REVIEW OF LITERATURE

One of the earliest investigations concerning torsional strength of reinforced concrete was carried out by C. R. Young, W. L. Seger and C. A. Hughes<sup>(21)</sup> in 1922 at the University of Toronto. They tested twelve beams of rectangular cross section. The beams included plain concrete, concrete reinforced with longitudinal bars only, and concrete reinforced with longitudinal bars and spirals.

Their conclusions were that longitudinal bars alone did little to increase the ultimate torsional resistance in a concrete beam, but that spiral reinforcement increased the torque capacity considerably.

Paul Andersen<sup>(1)</sup> presented the results of his experiments with concrete subject to torsion in 1935. He tested forty-eight beams, including circular cross sections of plain concrete, square cross sections reinforced with  $\frac{1}{2}$  inch square rods in each corner, square cross sections reinforced with  $\frac{1}{2}$  inch square corner rods and  $\frac{5}{32}$  inch round ties spaced at six inches and at three inches, and beams of square cross section reinforced with  $\frac{1}{2}$  inch square corner rods and  $\frac{5}{32}$  inch round forty-five degree spirals spaced at two and at three inches.

Andersen concluded that the shearing modulus of concrete is proportional to its ultimate strength, and that concrete subject to torsion fails in tension due to its low tensile strength. The addition of corner rods increases the torsional resistance of small cross sections but should not be relied upon in design, as the extra strength becomes less with larger cross sections. On the other hand, vertical

web reinforcement will increase the torsional resistance and should be considered in design; and the forty-five degree spiral is the most effective type of reinforcement.

In Andersen's second series of tests in pure torsion, which he completed in 1937<sup>(2)</sup> he tested twenty-four specimens of rectangular cross section. He used unreinforced specimens, specimens with only  $3/8$  inch corner rods, and specimens with  $3/8$  inch corner rods plus forty-five degree spirals. His conclusions were that the modulus of elasticity in shear of concrete is a direct function of the modulus of elasticity in compression; and that corner rods and spiral reinforcement do not influence the elastic torsional rigidity of rectangular beams. Andersen also stated that rectangular concrete sections subject to torsion fail near the center of the longest side, due to high tensile stresses in that region. He found that the square was the most efficient rectangular cross section to resist torsional stresses, and that the addition of corner rods did little to raise the member's torsional strength. Spiral reinforcement of an amount greater than one fourth of one per cent of the concrete volume could be relied upon to increase the torsional strength of concrete if it were securely fastened to the corner rods. Andersen also stated that the spiral reinforcement can be assumed to take most of the tensile stresses in excess of the ultimate tensile strength of the concrete.

H. L. Cowan<sup>(6,7,8,9,10)</sup> has done a considerable amount of work with reinforced concrete subject to pure torsion and combined bending and torsion. By using the general theory of torsion developed by

St.-Venant, Cowan obtains Equation (1) for the relation between the torque and maximum shear stress in a rectangular section:

$$M_c = \alpha b^2 d c_{max} \quad (1)$$

where

$M_c$  = torsional resistance of plain concrete

$\alpha$  = a hyperbolic function of  $d/b$

$b$  = width of rectangular section

$d$  = depth of rectangular section

$c_{max}$  = maximum allowable shear stress

St.-Venant's theory was again applied to obtain the stirrup strains in order to evaluate the added resistance of stirrup reinforcement. Then the energy stored in the reinforcement was equated to the work done by the twisting moment. The added moment is given by the equation

$$M_s = \lambda \frac{b' d'}{2} \frac{A_v}{s} f_v \quad (2)$$

where

$M_s$  = added moment due to stirrup reinforcing

$b'$  = width of reinforcing cage

$d'$  = depth of reinforcing cage

$A_v$  = cross section area of one bar

$f_v$  = allowable steel stress

$s$  = stirrup spacing

$\lambda$  = a hyperbolic function of  $d'/b'$

The sum of Equations (1) and (2) gives the torsional strength, in the

elastic range, of a rectangular beam reinforced with vertical closed stirrups.

To evaluate the ultimate strength of rectangular sections of concrete subject to torsion Cowan assumes full plasticity in the section. He then refers to Nadai,<sup>(16)</sup> who has shown the torsional resistance of a rectangular section in the plastic state to be

$$M_p = \frac{b^2}{2} \left( d - \frac{b}{3} \right) s \quad (3)$$

where

b = shorter side of rectangle

d = longer side of rectangle

s = shear stress

Since pure torsion causes compressive and tensile stresses numerically equal to the shear stress, the maximum shear stress for concrete is limited by its maximum tensile strength. Equation (2) for the contribution of reinforcement to the torsional moment is still valid. Therefore the ultimate torsional moment for a rectangular section of reinforced concrete is given by the sum of Equations (2) and (3). For a plain concrete beam only Equation (3) should be used.

In 1957 G. C. Ernst<sup>(11)</sup> conducted a series of experiments to determine the optimum amounts of longitudinal and transverse steel for rectangular reinforced concrete members in pure torsion at ultimate torque. Ernst used three longitudinal steel ratios, six transverse steel ratios, and one concrete strength. For the member to reach a plastic state at failure, enough longitudinal reinforcement must be

provided so that the ties will be able to resist the transverse component of the diagonal stresses. For the minimum amount of longitudinal steel Ernst gives the following equation:

$$A_L = 2 A_V \frac{(b' + t')}{s} \quad (4)$$

where

$A_L$  = total area of longitudinal steel placed symmetrically within the periphery of the reinforcing cage

$A_V$  = area of one bar of the transverse ties

$b'$  = width of reinforcing cage

$t'$  = depth of reinforcing cage

$s$  = stirrup spacing

If the area of the longitudinal steel is equal to or greater than that given by Equation (4), the plastic ultimate torque can be obtained from the following expression:

$$T_p = (k_v + k_h) \frac{A_V f_y}{s} b' t' \quad (5)$$

where

$T_p$  = plastic ultimate torque

$f_y$  = yield stress of the transverse ties

$k_v$  and  $k_h$  are factors which when multiplied by  $b'$  and  $t'$  respectively, represent the lever arm of the force in terms of the reinforcing cage dimensions.

$A_V$ ,  $s$ ,  $b'$ , and  $t'$  are the same as defined in Equation (4).

A comment on Ernst's equation (Equation (5)) for the ultimate torque may be appropriate here. While the equation may be in the correct form to predict the ultimate torsional capacity of a beam, the term  $(k_v + k_h)$  is unknown. Ernst made his experimental results fit the

equation by computing  $(k_v + k_h)$  from observed ultimate torques. For design purposes  $(k_v + k_h)$  has to be known, or a reasonable estimate made. Since  $k_v b'$  represents the lever arm of the force developed in the ties across the top (or bottom) of the beam, and  $k_h t'$  the lever arm of the force in the ties on the sides, one might think intuitively that the term  $(k_v + k_h)$  would seldom be much larger than 2.00. If it were, then the lever arms of the forces in the transverse ties would be longer than the dimensions of the member. Later tests by Shan<sup>(19)</sup> indicate that the lever arms must fall within the member. Therefore the maximum value of  $(k_v + k_h)$  would be 2.00, letting each coefficient equal 1.00. Ernst's computed values of  $(k_v + k_h)$  vary from 1.23 to 7.96.

E. Q. Shan<sup>(19)</sup> tested five reinforced concrete beams in pure torsion. The beams had four different combinations of longitudinal reinforcement as well as three different types of transverse reinforcement. The types of transverse reinforcement used were hoops, spirals and closed vertical stirrups.

Shan concluded that the elastic formulas (Cowan's) are dangerous to apply for working loads since the working load values he obtained were too close to the ultimate; that the parabolic stress distribution normally assumed in torsion problems is not applicable to ultimate torque theory; and that the concrete in compression should be considered in its plastic range. Shan also found that the most efficient type of reinforcement is transverse ties accompanied by longitudinal bars, and that neither is suitable alone. As stated previously, Shan concluded

that the lever arm that determines the point of rotation of the forces present in the transverse steel should lie within the member.

Professor Hans Gesund<sup>(12)</sup> of the University of Kentucky has directed experimental investigations in pure torsion and has also made an analytical study of the problem. Gesund found the failure mechanism shown in Fig. 1-1 to be valid, and used this mechanism to develop a failure theory as follows:

The concrete is assumed to be cracked and offers no tensile resistance to the torque. When the concrete cracks, there is a redistribution of stresses and the steel reinforcement takes up the load across the crack. The resistance offered by the reinforcing cage is assumed to be provided by four different actions: the tensile forces in the ties, the dowel action of the ties, the dowel action of the longitudinal steel, and the bending of the ties across the hinge (Fig. 2-1). If the compressive hinge forms on top of the beam and  $s$  is the spacing of the ties, the number of steel surfaces exposed by the failure surface will be

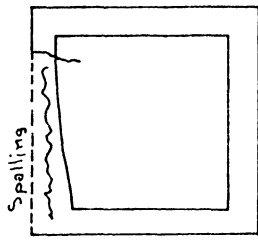
$$\frac{2 d_1 + b_1}{s} \quad (6)$$

where  $d_1$  and  $b_1$  are the depth and width of the reinforcing cage. The total torque resisted by the transverse ties in tension will be

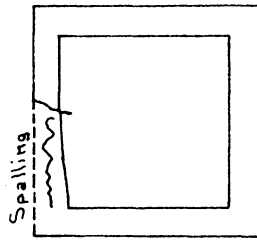
$$T_t = A_s f_{yt} \frac{2d_1}{s} \frac{b_1}{2} + A_s f_{yt} \frac{d_1}{s} b_1 = \frac{2 b_1 d_1}{s} A_s f_{yt} \quad (7)$$

where  $A_s$  is the area of one bar of the stirrup and  $f_{yt}$  the yield stress of the steel.

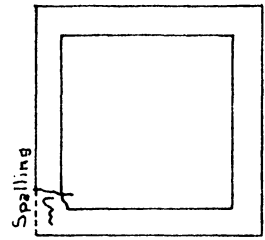
The resistance due to dowel action of the ties is more difficult



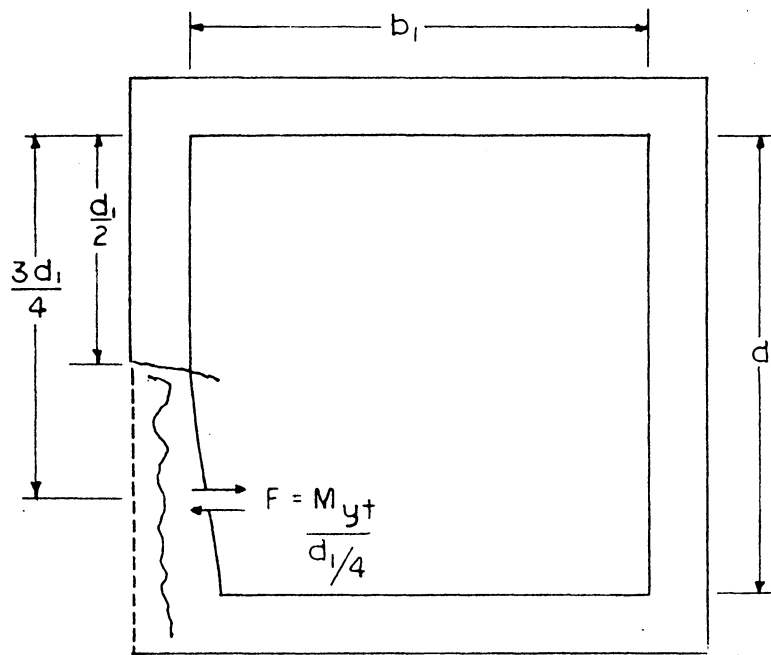
Long S-curve



Medium S-curve



Short S-curve



Median Tie

Figure 2-1 Example of Gesund's Dowel Action

to evaluate. The ties will tend to bend in an S-shape on the sides adjacent to the hinge and cause spalling of the concrete cover. The length of the S is difficult to determine, since the crack could cross the tie at any point. If the crack is assumed to be at forty-five degrees, and there are several stressed ties, the average length of the S-curve would be  $\frac{1}{2} d_1$ , assuming that the hinge formed on the top or bottom face of the beam. The bending resistance of the bar may be expected to be between the yield moment and the full plastic moment, lying closer to the yield moment since the deformations are small. If the beam contains only corner bars as longitudinal reinforcement, the dowel action can be determined by finding the torque supplied by the median tie and multiplying it by the number of ties affected. Therefore,

$$T_{td} = \frac{M_{yt}}{\frac{1}{2}d_1} \cdot \frac{3d_1}{4} \cdot \frac{2d_1}{s} = 6 M_{yt} \frac{d_1}{s} \quad (8)$$

where  $M_{yt}$  is the yield moment of the tie.

The longitudinal reinforcement also provides torsional resistance by dowel action. This can be handled in the same manner as the dowel action of the ties. The length of the S-curve in this case will be one half the spacing of the ties. Each longitudinal bar is affected once. For  $n$  longitudinal bars the resisting torque due to dowel action will be

$$T_{Ld} = \sum_1^n \frac{2 M_{yL}}{s} \cdot r \quad (9)$$

where  $M_{yL}$  is the yield moment of the longitudinal bar, and  $r$  is the perpendicular distance from the bar to the axis of rotation.

The last component to be considered as resisting the applied torque is the bending of the ties about the hinge (Fig. 2-1). The resisting torque of this component will be

$$T_{tb} = M_{yt} \cdot \frac{2 d_1 + b_1}{s} \quad (10)$$

The total torque that can be resisted by the reinforcing cage in pure torsion is the sum of these four quantities:

$$T_{total} = \frac{2 b_1 d_1}{s} A_s f_{yt} + 6 M_{yt} \frac{d_1}{s} + \sum_1^n \frac{2 M_{yL}}{s} \cdot r + M_{yt} \cdot \frac{2 d_1 + b_1}{s} \quad (11)$$

Ernst's and Gesund's analyses and resulting equations are based on the assumption that the reinforcing steel provides the total resisting torque and that both the longitudinal and transverse steel must yield before ultimate failure can take place. It would seem that there could be conditions of failure where all the steel does not yield, as for example, when

- 1) only the longitudinal steel yields and the strength of the transverse steel is not fully developed;
- 2) only the transverse steel yields and the strength of the longitudinal steel is not fully developed;
- 3) the concrete first fails in shear between the ties; or
- 4) the concrete first crushes in compression.

Such failures would not be correctly evaluated by Equations (5) and (11). Whether or not these equations could be modified to include other conditions of failure will require more study.

### III. EXPERIMENTAL WORK AND RESULTS

#### A. Experimental Work.

There were eight beams tested in this series. Each beam was 4'-6" long, with a 2'-6" long test section in the middle. All of the beams had the same cross section (8" x 8"), and the same amount of longitudinal steel (4 No. 3 bars, one bar in each corner). The spacing of transverse reinforcing ties was varied for each pair of beams; No. 3 stirrups were placed at 2", 4" and 6" spacing in each of three pairs; no stirrups were used in a fourth pair (Table 1).

All the reinforcing was ASTM - A - 305 deformed hard grade steel No. 3 bars, and was obtained from a local supply company.\* A representative sample of the reinforcing steel was tested in tension, and the yield strength was found to be approximately 50,000 psi.

The concrete used in these tests was obtained from a local ready-mix plant\*\* and contained the following quantities per cubic yard:

Portland Cement (Type I)	522 lbs.
Sand	1522 lbs.
No. 57 crushed stone (Maximum size 3/4")	1508 lbs.
Water	374 lbs. (approx.)

Water was added in the mix-truck. A relatively stiff mix was obtained with a slump of less than 2" for the beams of group 1, and a slump of

---

\*Valley Steel Corporation, Salem, Virginia.

\*\*Blacksburg Block and Supply Company, Blacksburg, Virginia.

**TABLE 1**  
**Properties of Test Beams**

BEAM	TIE SPACING (Inches)	AGE AT TEST (Days)	CONCRETE CYLINDER STRENGTH (PSI)	MODULUS OF ELASTICITY (PSI)
1-1	2	58	6301	$5.35 \times 10^6$
1-2	4	40	6301	$5.35 \times 10^6$
1-3	6	54	6301	$5.35 \times 10^6$
1-4	No Ties	51	6301	$5.35 \times 10^6$
2-1	2	62	5320	$4.84 \times 10^6$
2-2	4	55	5320	$4.84 \times 10^6$
2-3	6	59	5320	$4.84 \times 10^6$
2-4	No Ties	69	5320	$4.84 \times 10^6$

All reinforcement consists of No. 3 bars.

All beams have 4 No. 3 bars as longitudinal reinforcement (one in each corner).

2½" - 3" for the beams in group 2. This mix and the materials used meet the minimum requirements of the Virginia State Highway Department for a six bag mix.

The eight beams were cast in two pours of concrete one week apart. Six standard test cylinders, used to determine the modulus of elasticity and the ultimate strength, were taken from each pour.

The beams and control cylinders were cured four days in the forms under wet burlap. At the end of this period the forms were stripped and the cylinders and beams placed in a one hundred per cent humidity curing room. The beams stayed in the curing room until two or three days before the tests. They were then moved to the testing laboratory and allowed to air dry at normal room temperature and humidity. After the surfaces were sufficiently dry, the strain rosettes were mounted using Epoxy - 150 cement.\* The control cylinders and beams were in the curing room a minimum of thirty-five days. The age of the earliest beam tested was forty days.

To obtain a measure of the concrete strength, the control cylinders were tested in compression; the ultimate strengths were averaged for each pour. Individual test values varied +619 psi, -640 psi from the average. Table 1 gives the properties of each beam and the average cylinder strength. The average for pour number one is based on the results of five cylinder tests (one cylinder was damaged), that of pour two on six cylinder tests.

---

\*Baldwin-Lima-Hamilton Corporation, Electronics Division, Waltham, Massachusetts.

SR-4 Type FAB-25-12 electrical resistance strain gages were used to measure the strains in the reinforcing steel. These are wire gages mounted in a bakelite body. Before each gage was mounted on a bar, the bar deformations over a small area were removed using a hand file, and the area was polished using a fine emery cloth. This polished area was only slightly larger than the gage itself, and the change in bar diameter and cross sectional area was negligible (the reduction in area was less than 0.75%). After the gage was mounted and the cement had set for twenty-four hours, the lead-out wires were soldered to the gage leads. The entire installation was then water-proofed by brushing hot wax on and around the gage until the gage, bar and soldered connections were covered sufficiently to prevent any moisture from penetrating and causing a short circuit. A minimum of bar area was waxed to reduce the effect of loss of bond strength. Figures 3-2 and 3-3 show the gage before and after waxing.

SR-4 Type AR-2 45° strain rosettes were used to measure the concrete strains simultaneously in three directions. The concrete surface was rubbed smooth with a rubbing stone and dusted thoroughly before the gages were applied. The rosettes can be seen near the middle of the beams in the photographs of the failure surfaces (see Fig. 3-38, for example).

The strain gages used had the following characteristics:

Type	Gage Factor	Resistance (Ohms)	Cement Used
FAB-25-12	2.13	120	Epoxy-150
AR-2	2.06	119.5	Epoxy-150

The location of the strain gages on the reinforcing steel is shown in Figures 3-5 through 3-12. These figures are drawn so that the right side of the figure corresponds to the movable head on the testing machine. The machine head rotates clockwise when viewed from the right end.

The beams were tested in a Tinius-Olsen gear-driven beam balance torsion machine with a rated capacity of 60,000 inch-pounds. The maximum load applied during testing was 76,000 inch-pounds, representing a twenty-seven per cent overload. The machine performed satisfactorily during all the tests. Special chucks were fabricated to hold the beams in the machine heads. These can be seen in Figure 3-4. The beam ends were placed in the chucks (which were one fourth inch larger than the beam's cross sectional dimensions), and plaster of Paris was packed around the ends of the beam to prevent the irregularities of the chuck from causing stress concentrations.

The strain indicating equipment consisted of two Baldwin Gage Selectors with twelve channels each, and two Baldwin Strain Indicators (Model M). The strains were recorded to the nearest micro-inch per inch.

At the beginning of each test the strain indicators were adjusted using the potentiometers on the twelve channel gage selectors to place the initial gage readings in the mid-range of the equipment. A small initial torque of approximately 100 inch-pounds was applied, initial gage readings were set and the torque then increased in increments of approximately 5,000 inch-pounds until failure. Strain gage

AUG • 63



Figure 3-1 Beams Curing in the Forms

• AUG • 63

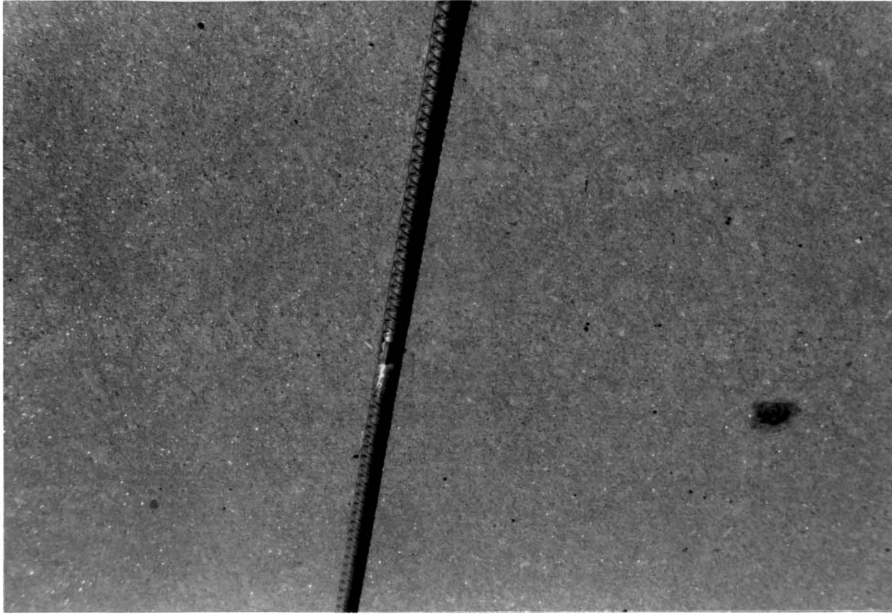


Figure 3-2 Strain Gage Before Waxing

• AUG • 63

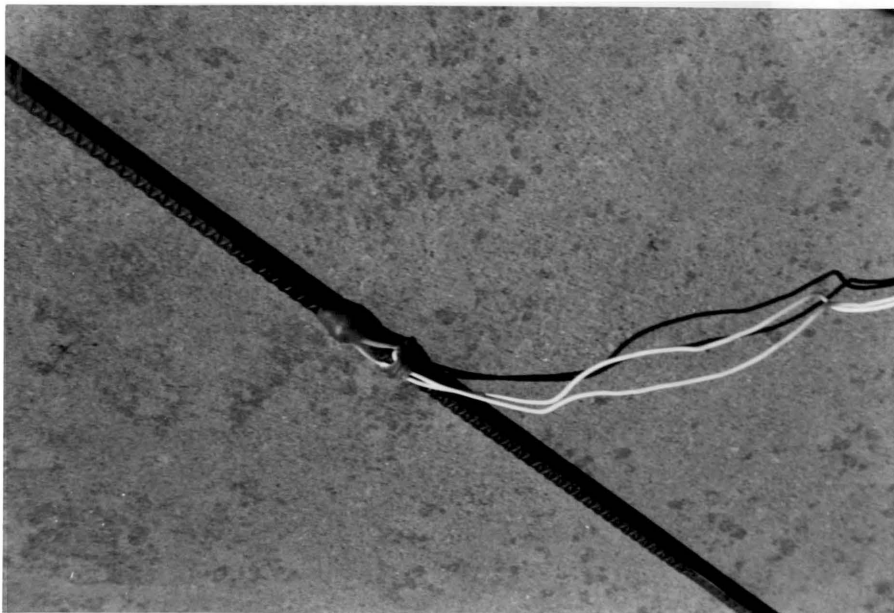
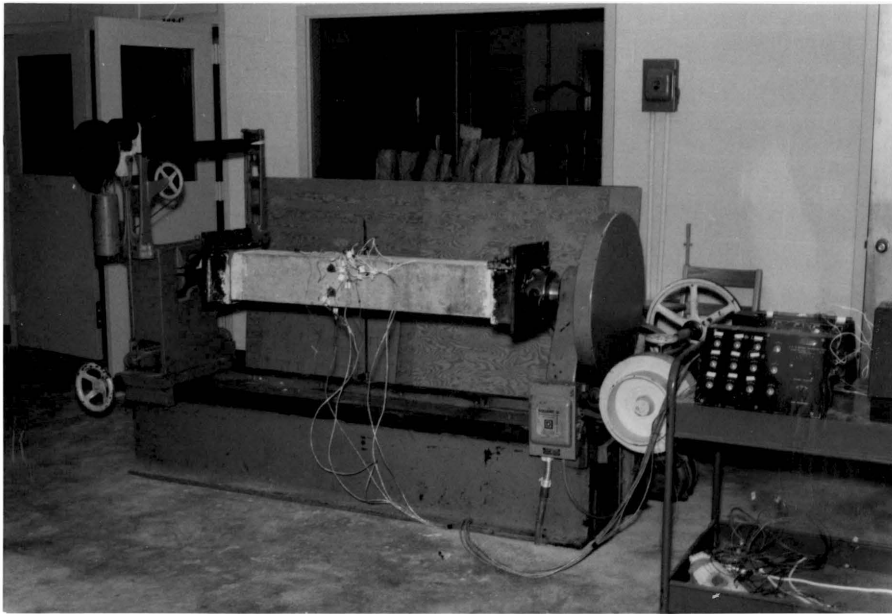


Figure 3-3 Strain Gage After Waxing



AUG • 63

Figure 3-4 General Testing Arrangement

readings were recorded after each torque increment was applied. After failure, additional torque was applied to develop the crack pattern fully for visual study.

Three persons assisted in conducting the tests. The testing machine was operated manually, making it easier to maintain the proper loading increment. One person operated the machine, and then read and recorded the steel strains. The second person balanced the torque indicator arm, and observed and marked the crack patterns, while the third person read and recorded the concrete strains. In addition the first and second persons also measured the rotation at each end of the beam.

#### B. Results.

Beam 1-2 was the first specimen tested. The failure was characterized by numerous cracks forming continuously throughout the test, with no single crack predominating or widening as the torque increased. Failure was not sudden. As torque increased, a level was finally reached where the beam would no longer resist additional torque.

Each of the other seven beams failed very suddenly with little warning. Prior to failure few if any large cracks had formed. A few seconds before failure there was noticeable creep, accompanied by audible popping. The failure mechanism was similar to that shown in Figure 1-2. However, the compressive hinge was not noticeable until considerable twist was applied.

The results of the tests are given in Figures 3-13 through 3-45.

In Figures 3-13 through 3-24 the steel strains versus torque are plotted for each beam. The failure torque for each beam is noted on each figure. The steel strains increased rapidly with increased twist after the failure torque was reached and the resistance dropped off. Where the strains extend beyond the limits of the graph, this is indicated by an arrow. The slope of the arrow has no significance. The strain at maximum torque is recorded near the end of each line. Initial strains due to the dead weight bending were not recorded and are not included on the plots of data.

The strain rosettes gave the strains in three directions at each point. The principal tensile strain was computed by applying the following equation involving these strains:

$$e_t = \frac{e_x + e_y}{2} + \sqrt{\left(\frac{e_x - e_y}{2}\right)^2 + \left(\frac{e_g}{2}\right)^2} \quad (12)$$

where

$e$  = maximum tensile strain

$e_x$  and  $e_y$  = strains at right angles

$e_g$  = shearing strain computed from  $e_g = 2 e_{450} - (e_x + e_y)$

where  $e_{450}$  = the strain  $45^\circ$  from  $e_x$  and  $e_y$

The angle of the principal tensile strain ( $\theta$ ) was found using the following equation:

$$\tan 2 \theta = \frac{e_g}{e_x - e_y} \quad (13)$$

The angle of the principal tensile strain versus the torque is plotted for each beam in Figures 3-25 through 3-28. Figures 3-30

through 3-45 show the crack pattern and failure mechanism for each beam, with the predominating crack shown as a heavy line and the cracks of lesser magnitude as broken lines.

The total angular displacement of the test beams was measured and is plotted on Figure 3-29. No data were obtained for Beam 1-2. Data for Beams 1-1, 1-3, 1-4 and 2-2 were obtained from the indicator scale on the torsion machine which measured the rotation of one end chuck relative to the other. Data for Beams 2-1, 2-3 and 2-4 were obtained by measuring the deflections of horizontal extension arms attached near the ends of the beams.

During the test of Beam 2-2, it was noticed that the plaster of Paris filler in the end chucks was crumbling and the rotation data from the machine indicator were considered invalid. Therefore the system of extension arms was used for the last three beams tested.

An analysis of the predicted rotation using St.-Venant's principle<sup>(20)</sup> indicates that only the data for the last three beams can be considered valid. Assuming elastic action and neglecting the effect of the reinforcing on the modulus of elasticity and the moment of inertia of the section, St.-Venant's principle can be stated:

$$\theta = \frac{M_t L}{\beta b c^3 G}$$

where

$\theta$  = total angular displacement of the beam

$M_t$  = applied torque

$L$  = beam length

$\beta$  = a constant dependent upon  $b/c$

b = longer side dimension

c = shorter side dimension

G = shearing modulus =  $\frac{E}{2(1 + \mu)}$

E = modulus of elasticity

$\mu$  = Poisson's ratio

For these test beams:

$M_t$  = applied torque

L = 48" between extension arms

$\beta$  = 0.141

b = 8"

c = 8"

E = 4,840,000 psi

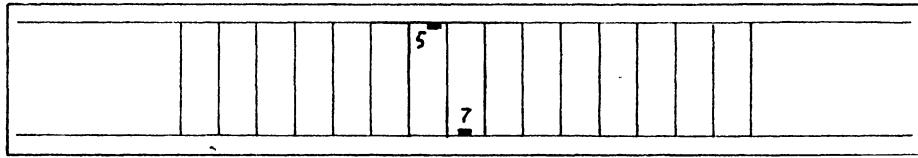
$\mu$  = 0.17

G = 2,060,000 psi

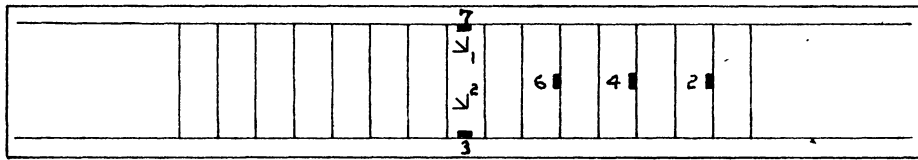
and

$$\theta = \frac{40000(48)}{(0.141) 8 (8)^3 2.06(10)^6} = .0016 \text{ radians} = .0922 \text{ degrees}$$

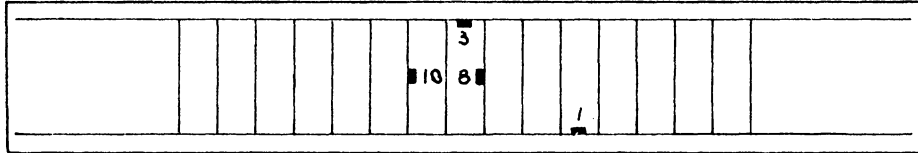
It is evident that the data for the last three beams are reasonably valid and verified by these computations, based on elastic action of the beam up to the cracking load. It is also evident that there was considerable slip in the end chucks as the plaster of Paris yielded under the pressures of the applied torque.



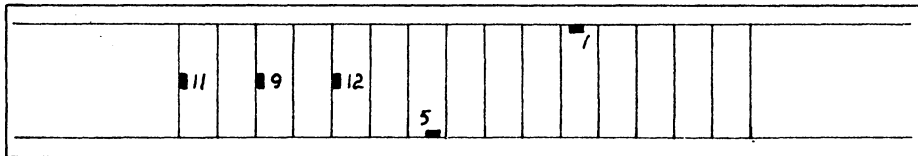
Top



Side



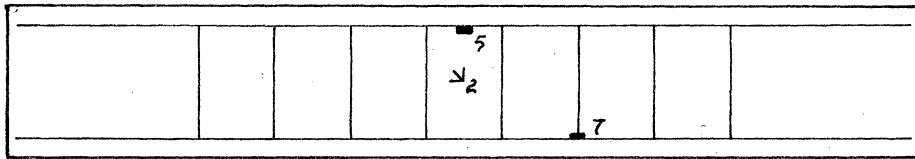
Bottom



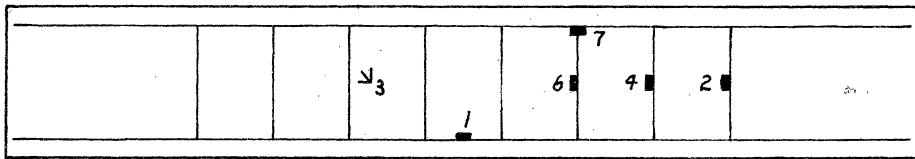
Side

∇ - Rosette Gage

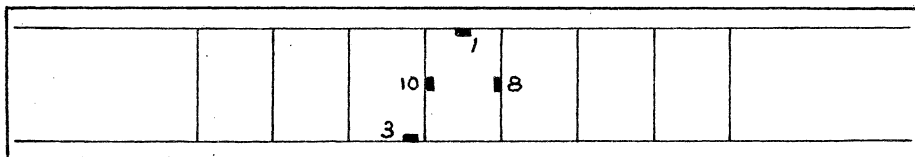
Figure 3-5 Strain Gage Locations, Beam 1-1



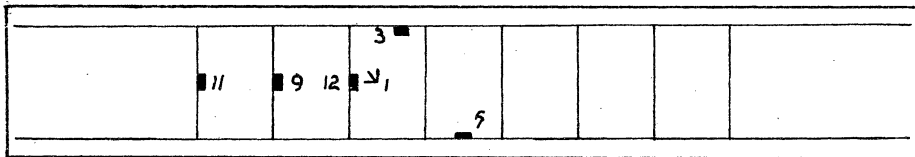
Top



Side



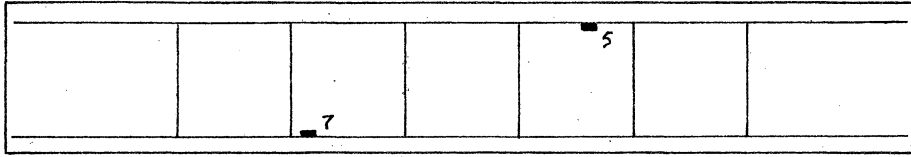
Bottom



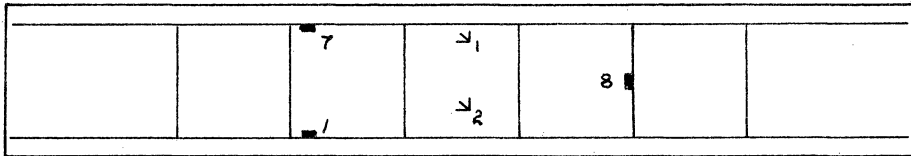
Side

∇- Rosette Gage

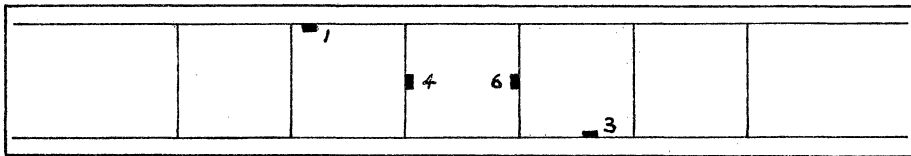
Figure 3-6 Strain Gage Locations, Beam 1-2



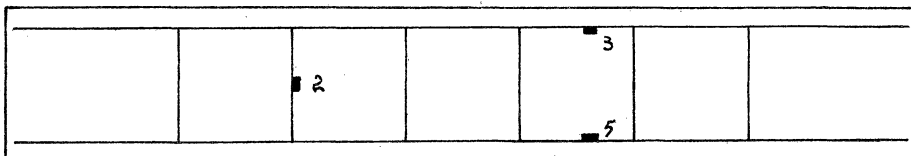
Top



Side



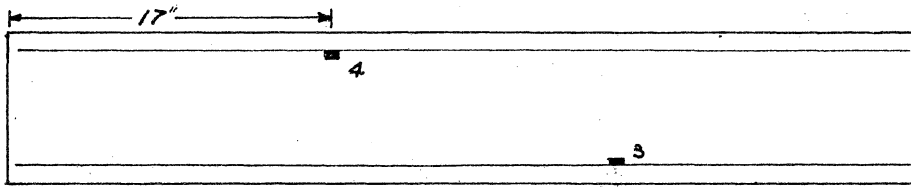
Bottom



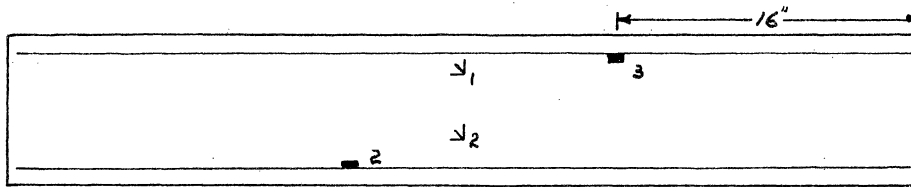
Side

Δ - Rosette Gage

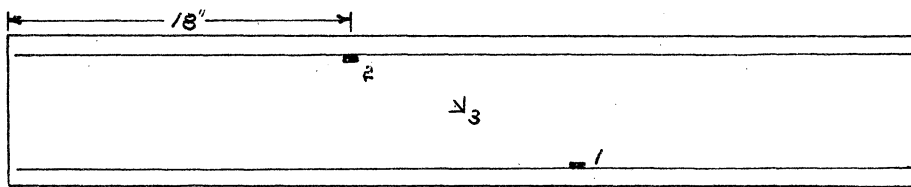
Figure 3-7 Strain Gage Locations, Beam 1-3



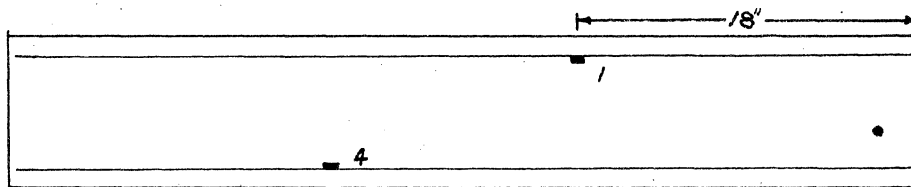
Top



Side



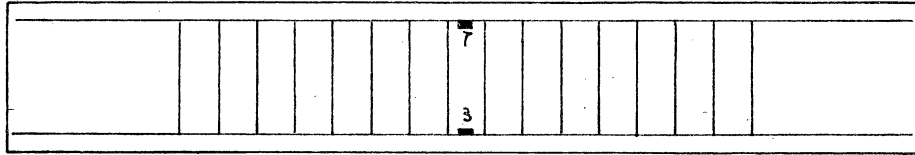
Bottom



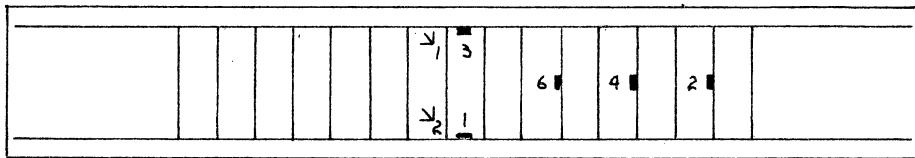
Side

∇ - Rosette Gage

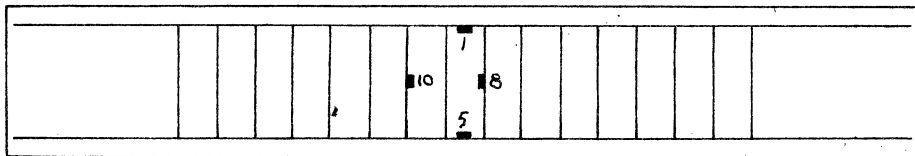
Figure 3-8 Strain Gage Locations, Beam 1-4



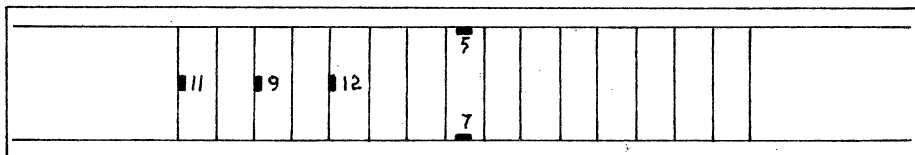
Top



Side



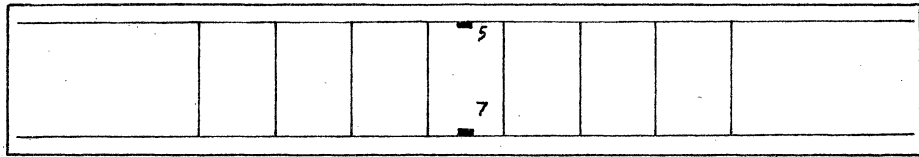
Bottom



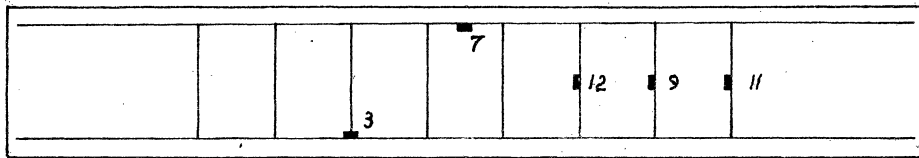
Side

▽ - Rosette Gage

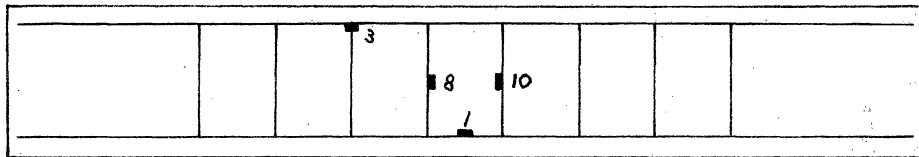
Figure 3-9 Strain Gage Locations, Beam 2-1



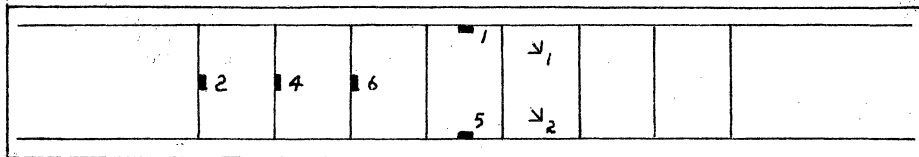
Top



Side



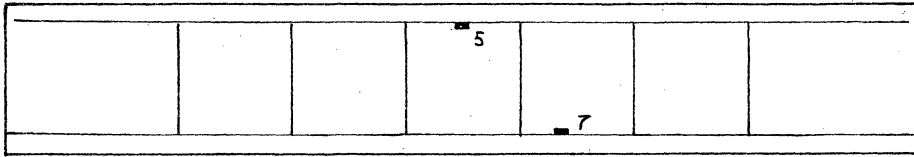
Bottom



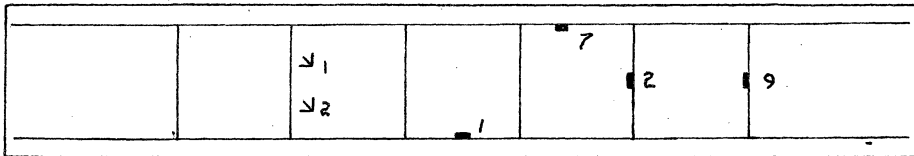
Side

∇ - Rosette Gage

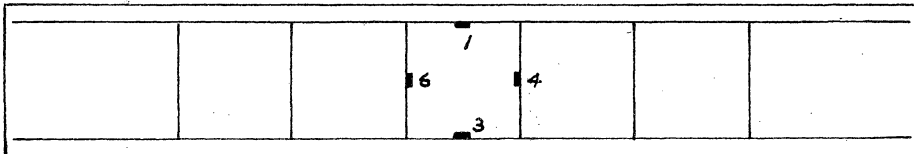
Figure 3-10 Strain Gage Locations, Beam 2-2



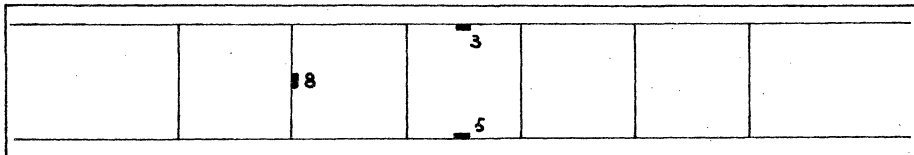
Top



Side



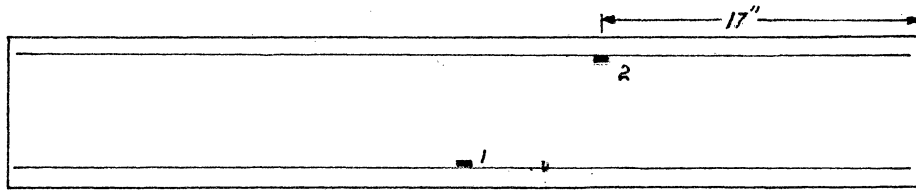
Bottom



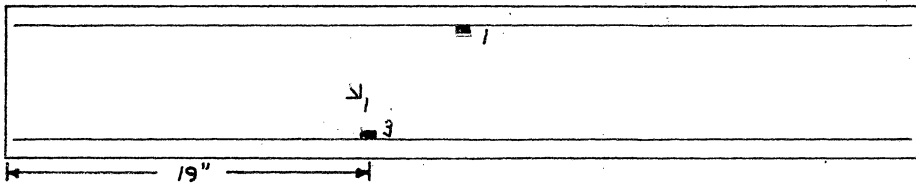
Side

∇ - Rosette Gage

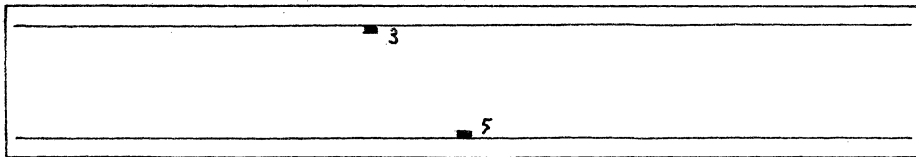
Figure 3-11 Strain Gage Locations, Beam 2-3



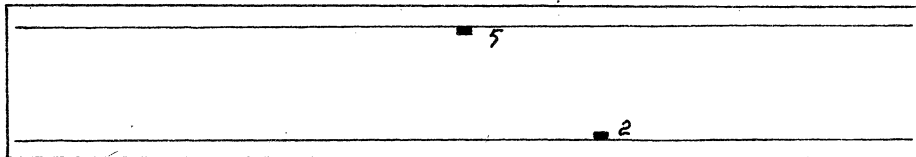
Top



Side



Bottom



Side

∇- Rosette Gage

Figure 3-12 Strain Gage Locations, Beam 2-4

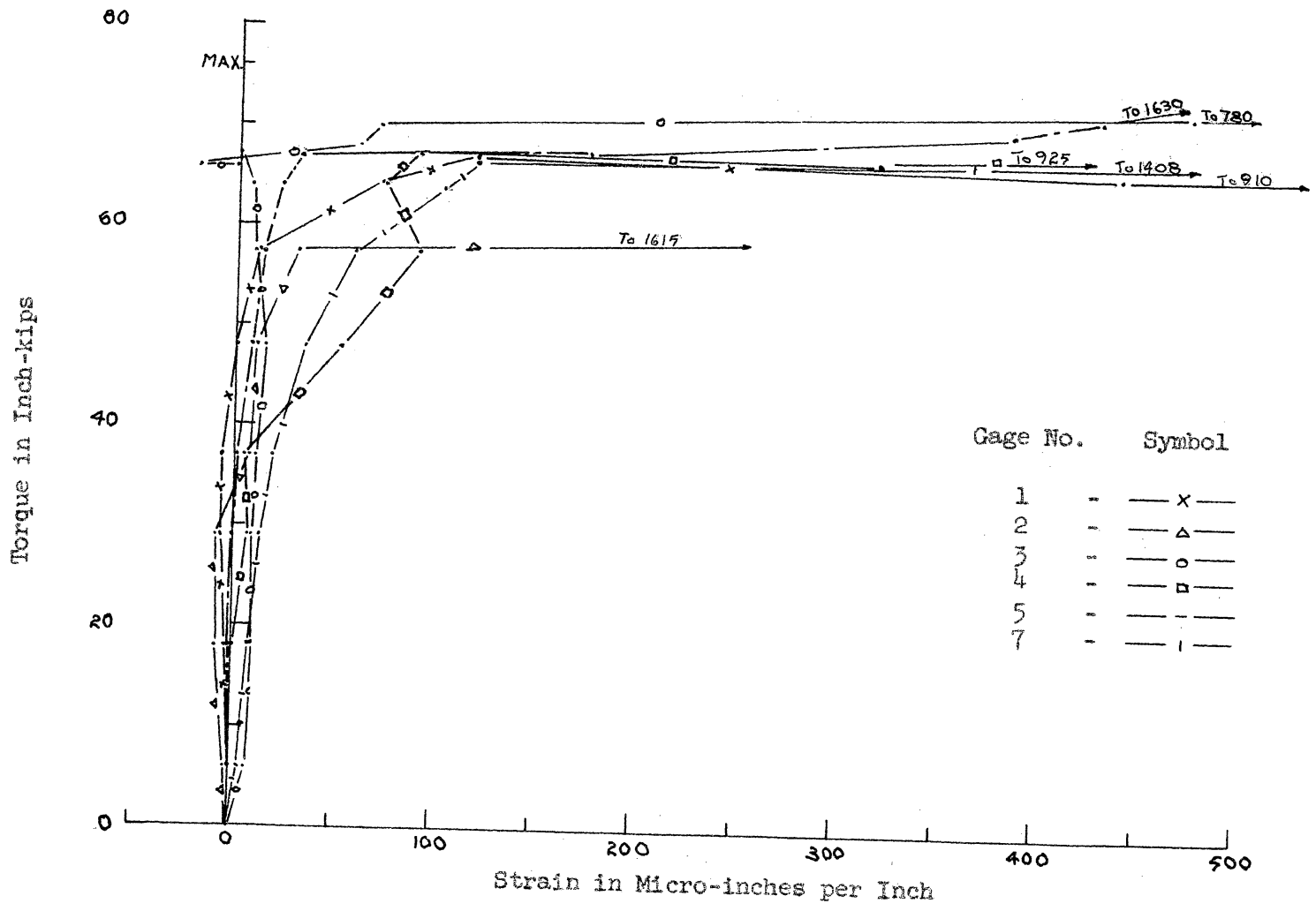


Figure 3-13 Torque - Strain Plot, Beam 1-1

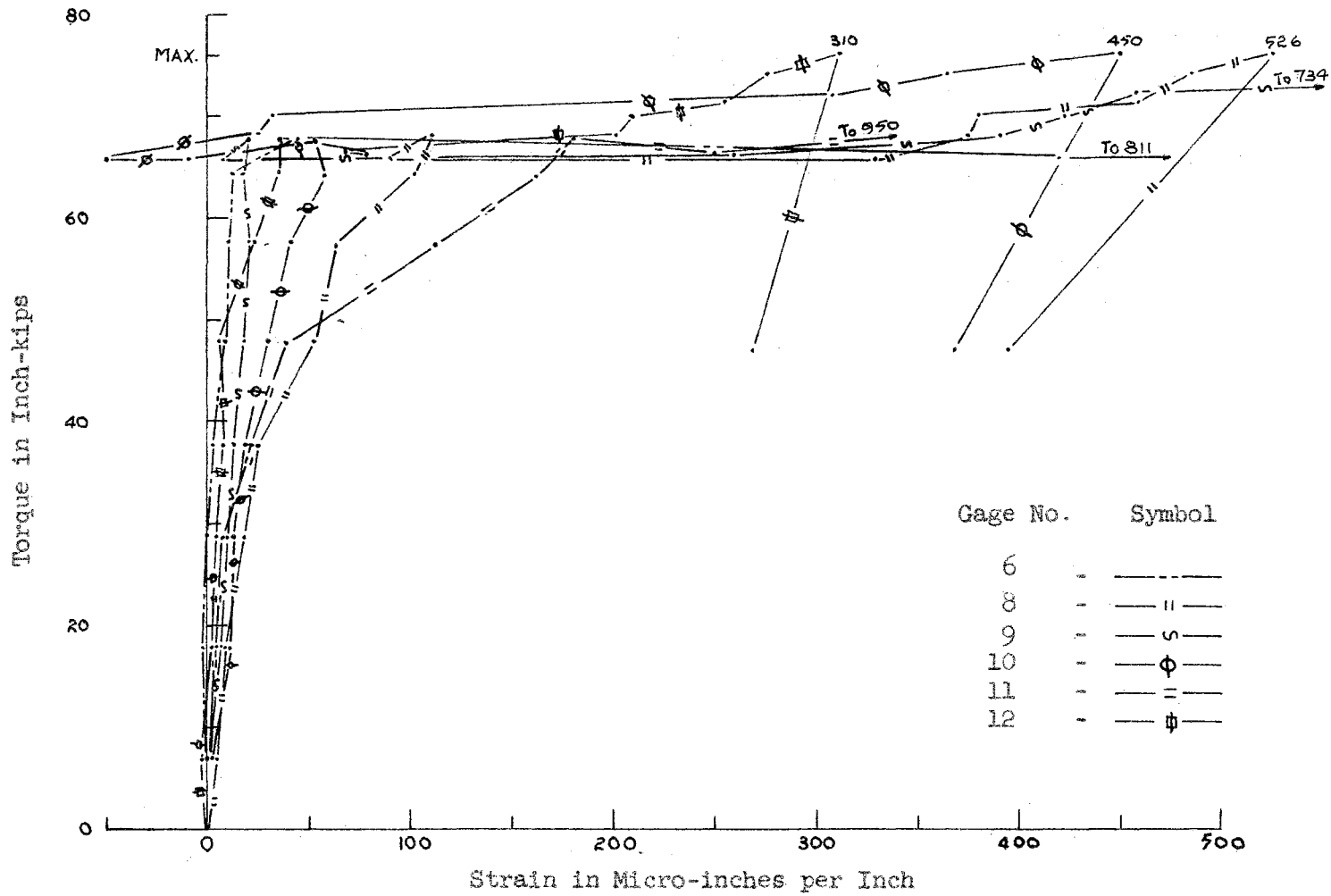


Figure 3-14 Torque - Strain Plot, Beam 1-1

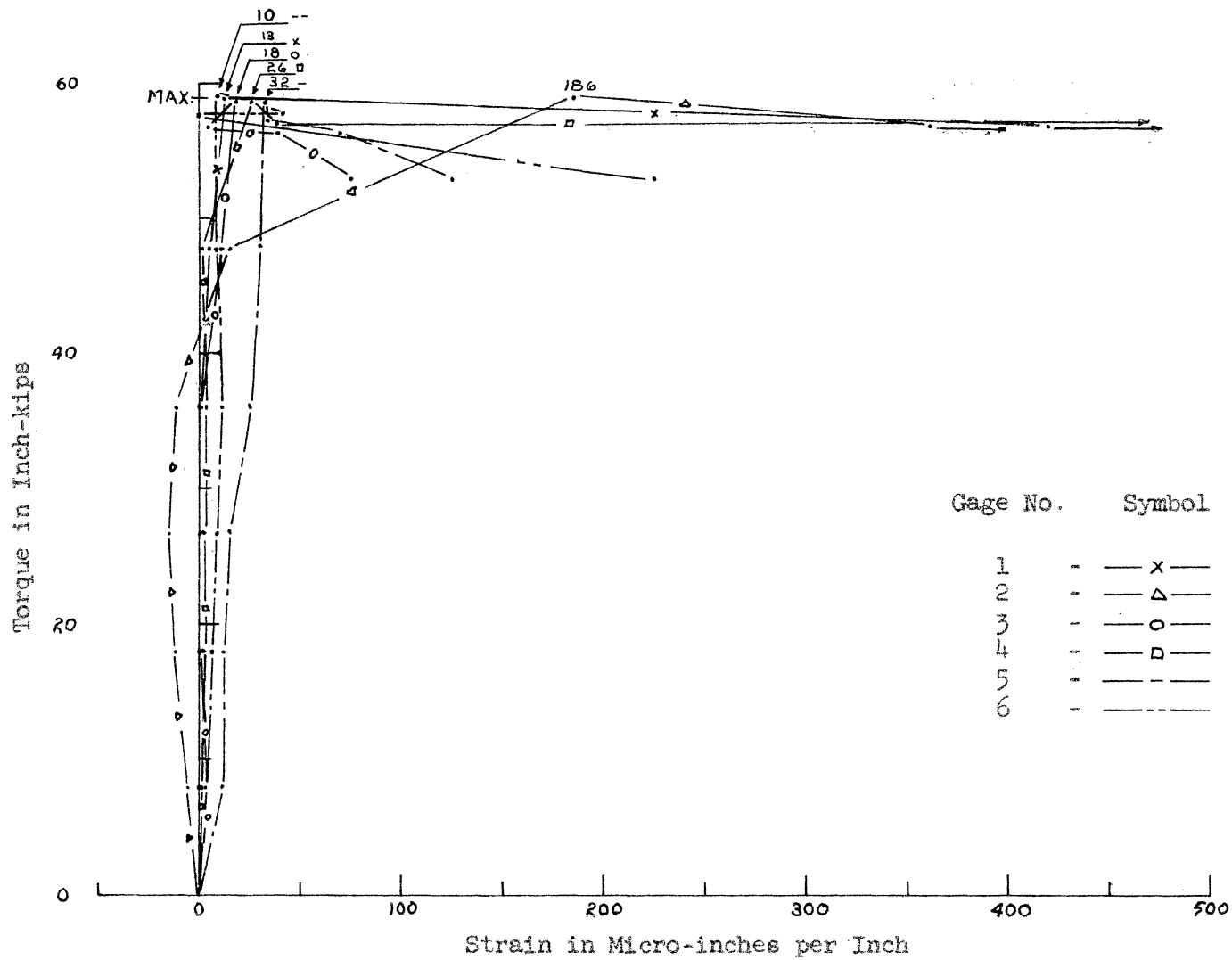


Figure 3-15 Torque - Strain Plot, Beam 1-2

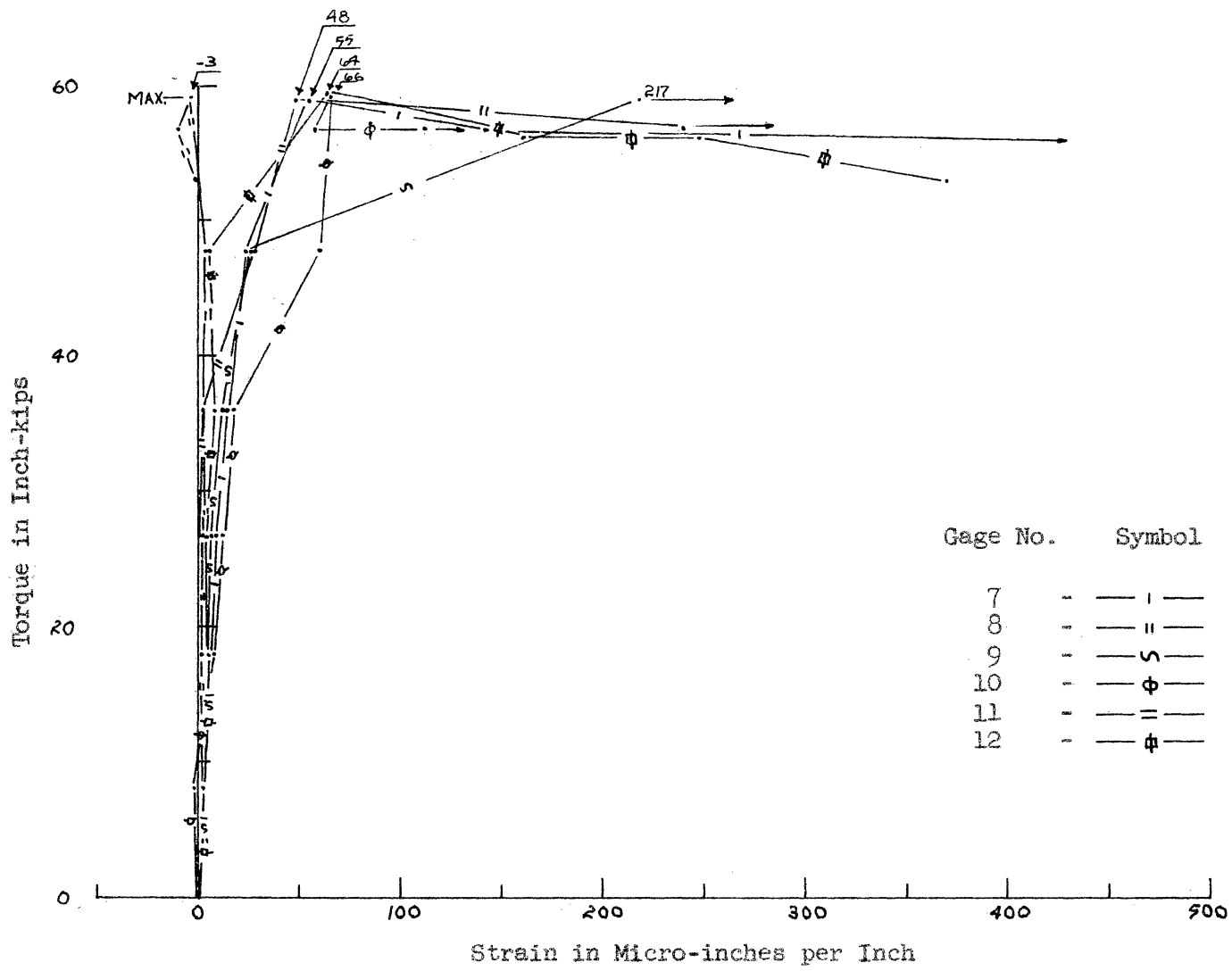


Figure 3-16 Torque - Strain Plot, Beam 1-2

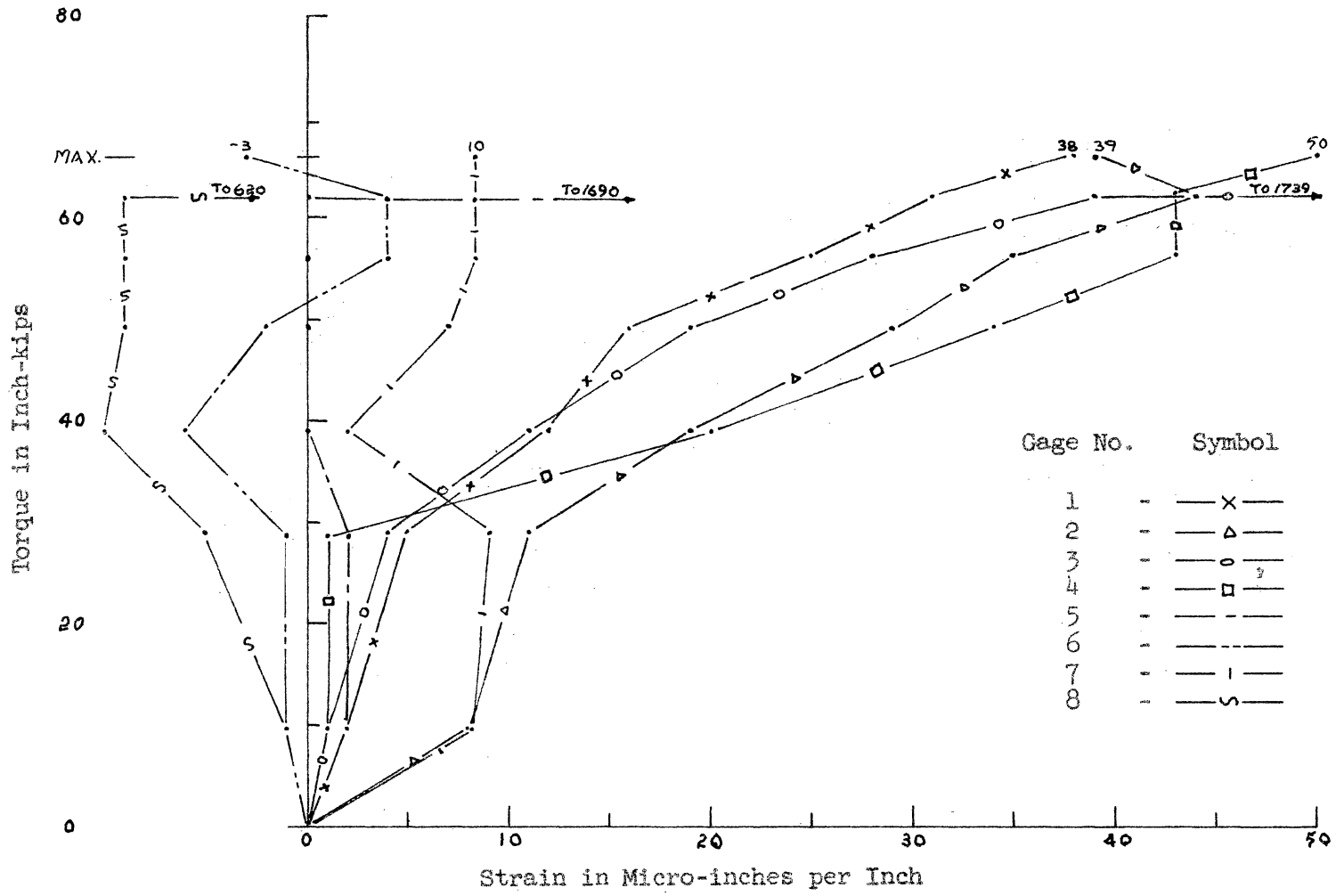


Figure 3-17 Torque - Strain Plot, Beam 1-3

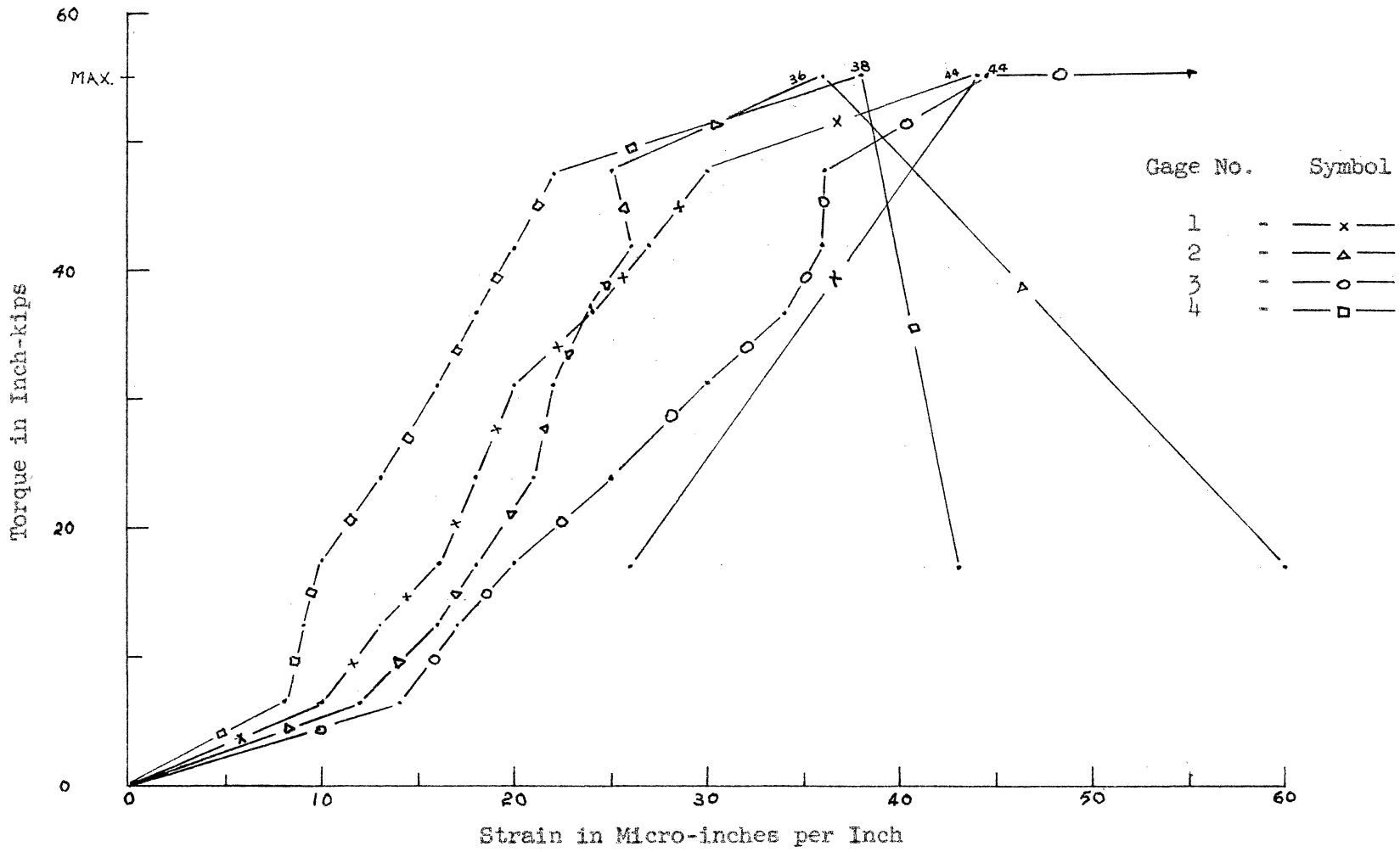


Figure 3-18 Torque - Strain Plot, Beam 1-4

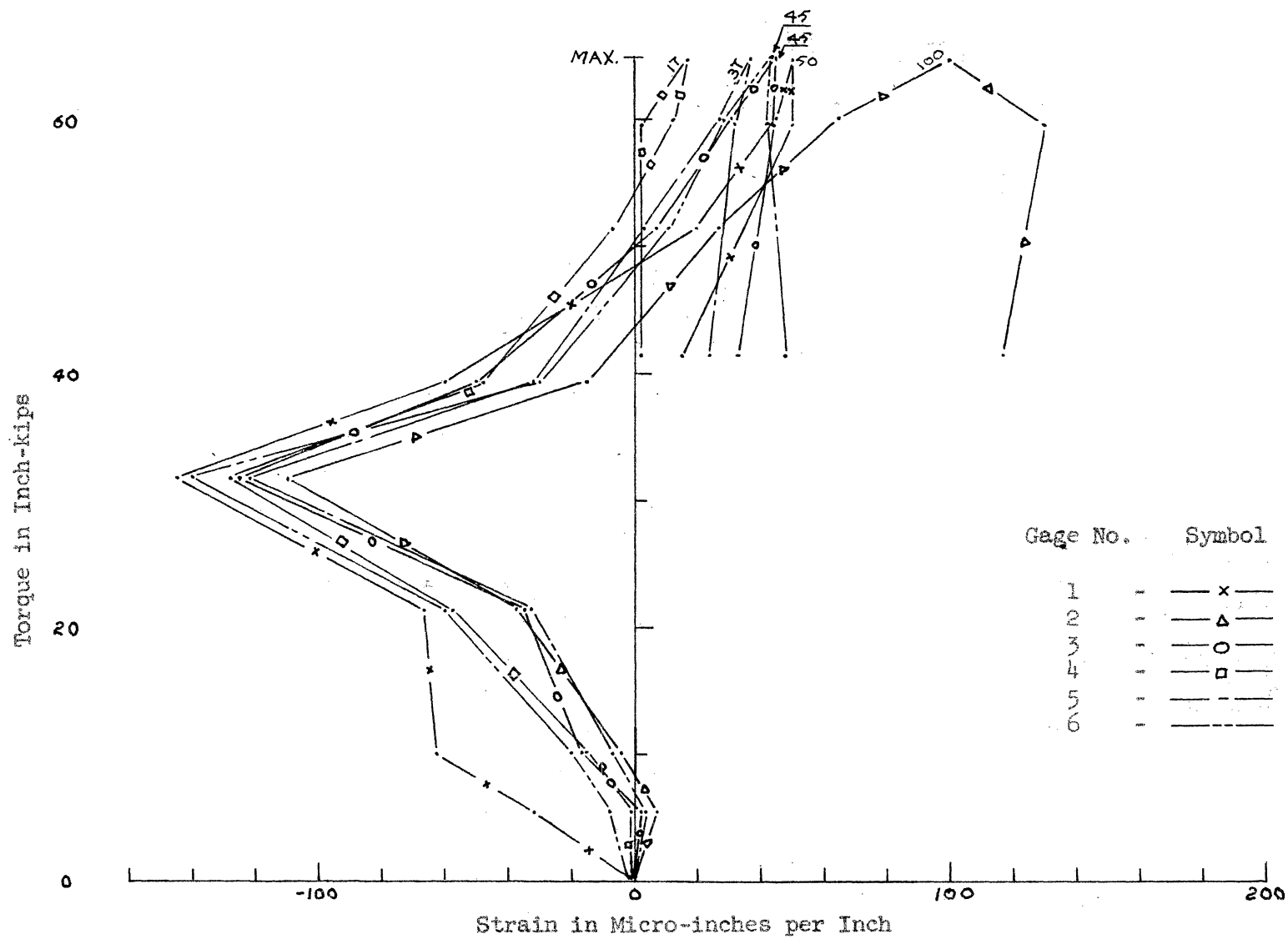


Figure 3-19 Torque - Strain Plot, Beam 2-1

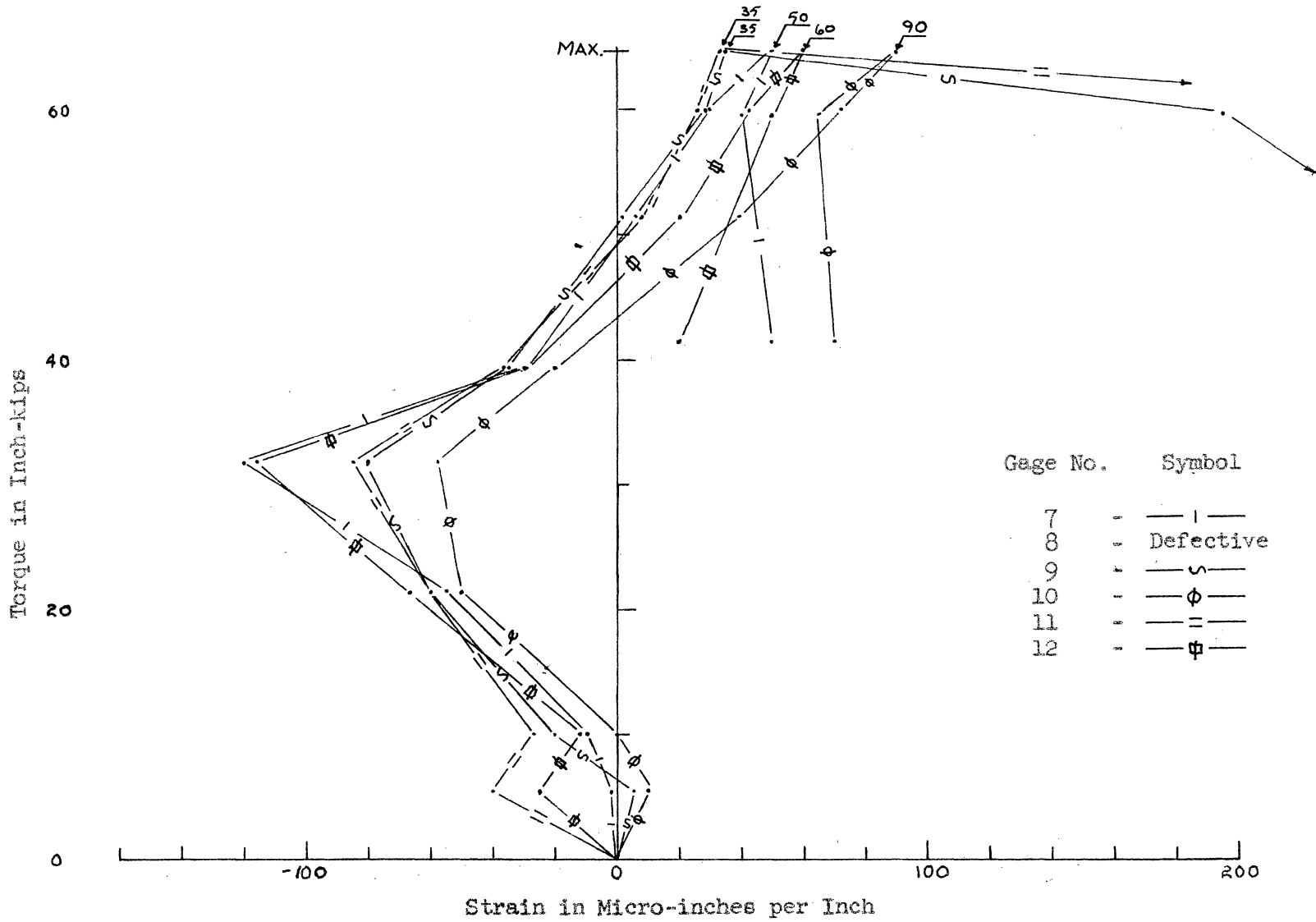


Figure 3-20 Torque - Strain Plot, Beam 2-1

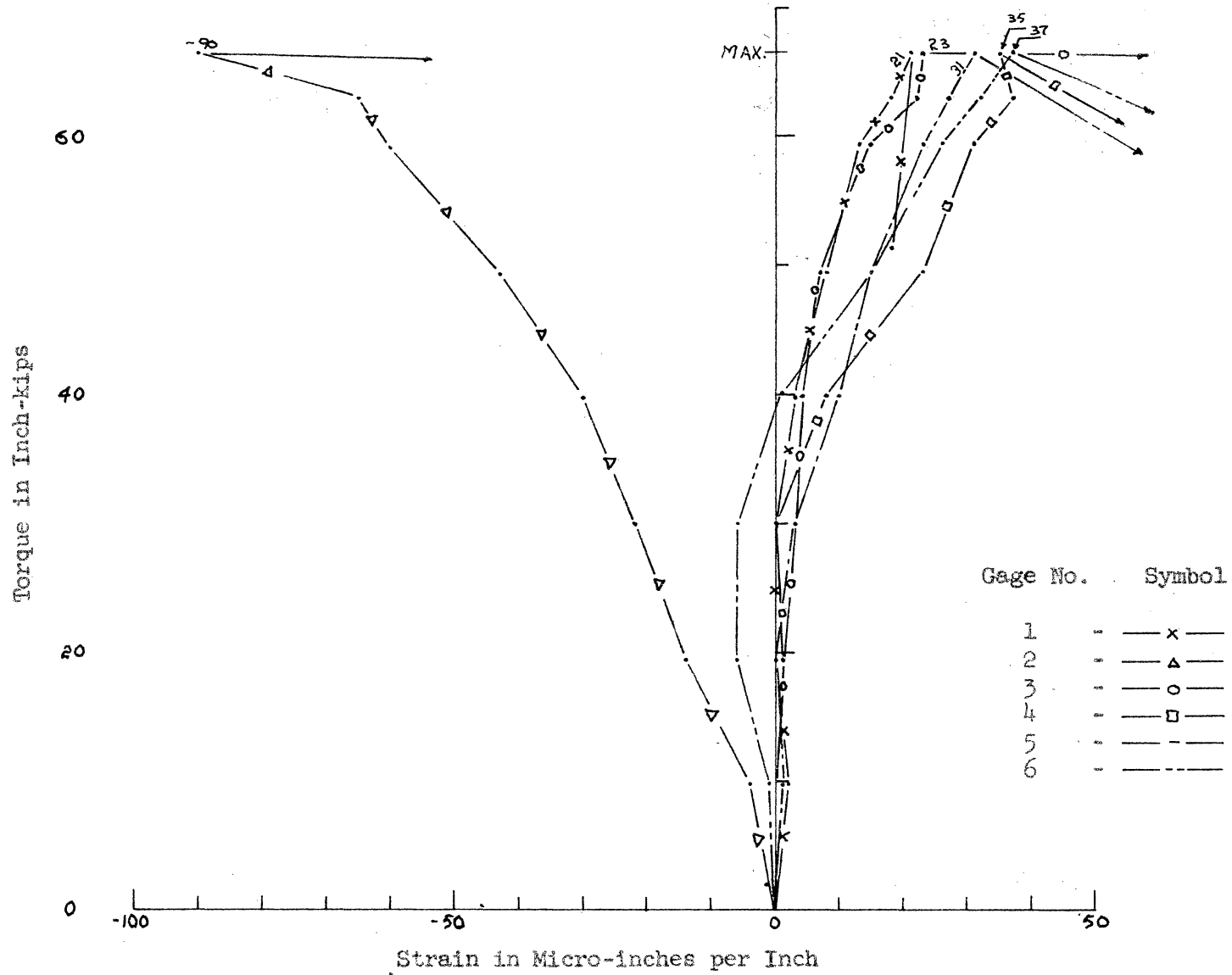


Figure 3-21 Torque - Strain Plot, Beam 2-2

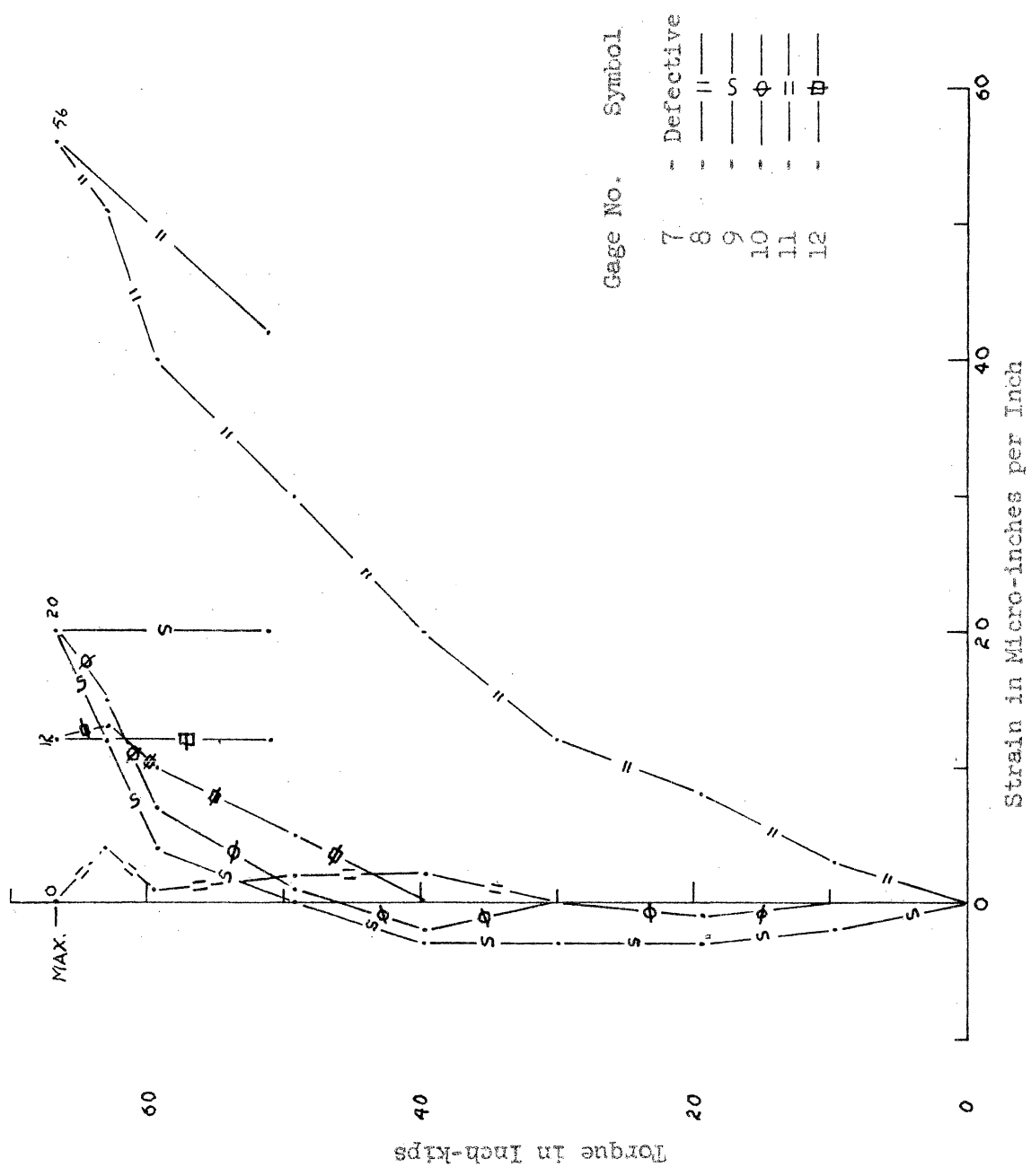


Figure 3-22 Torque - Strain Plot, Beam 2-2

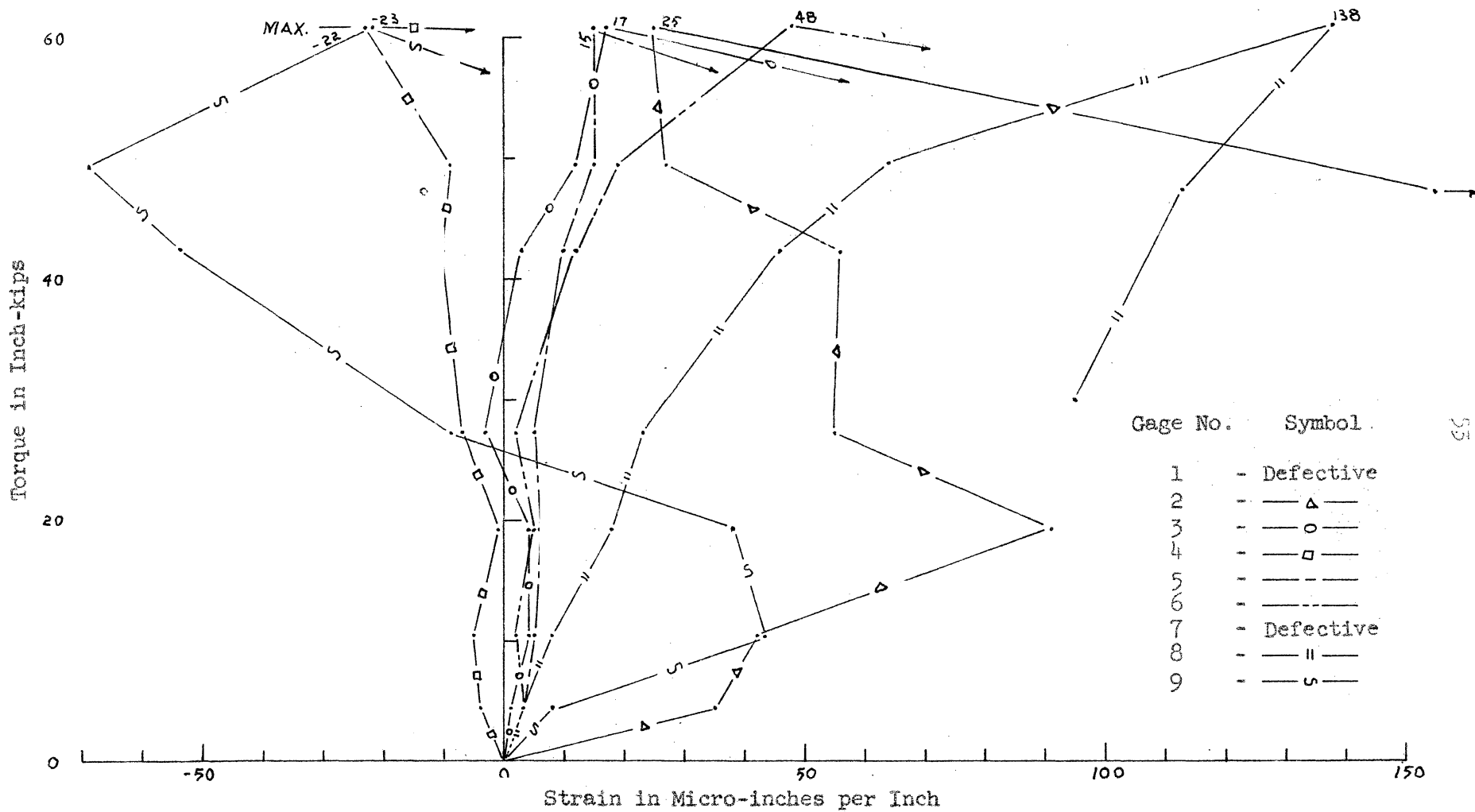


Figure 3-23 Torque - Strain Plot, Beam 2-3

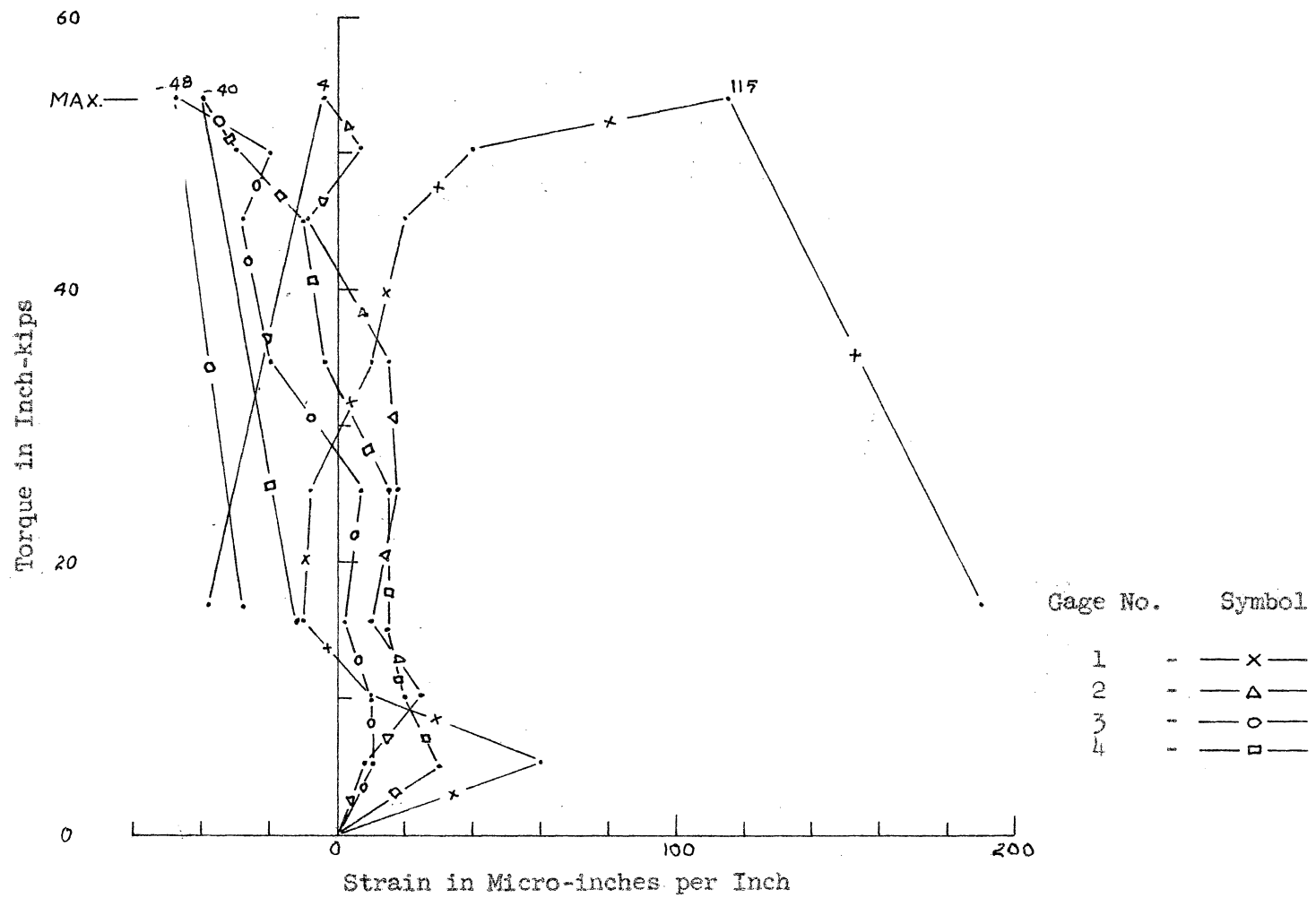


Figure 3-24 Torque - Strain Plot, Beam 2-4

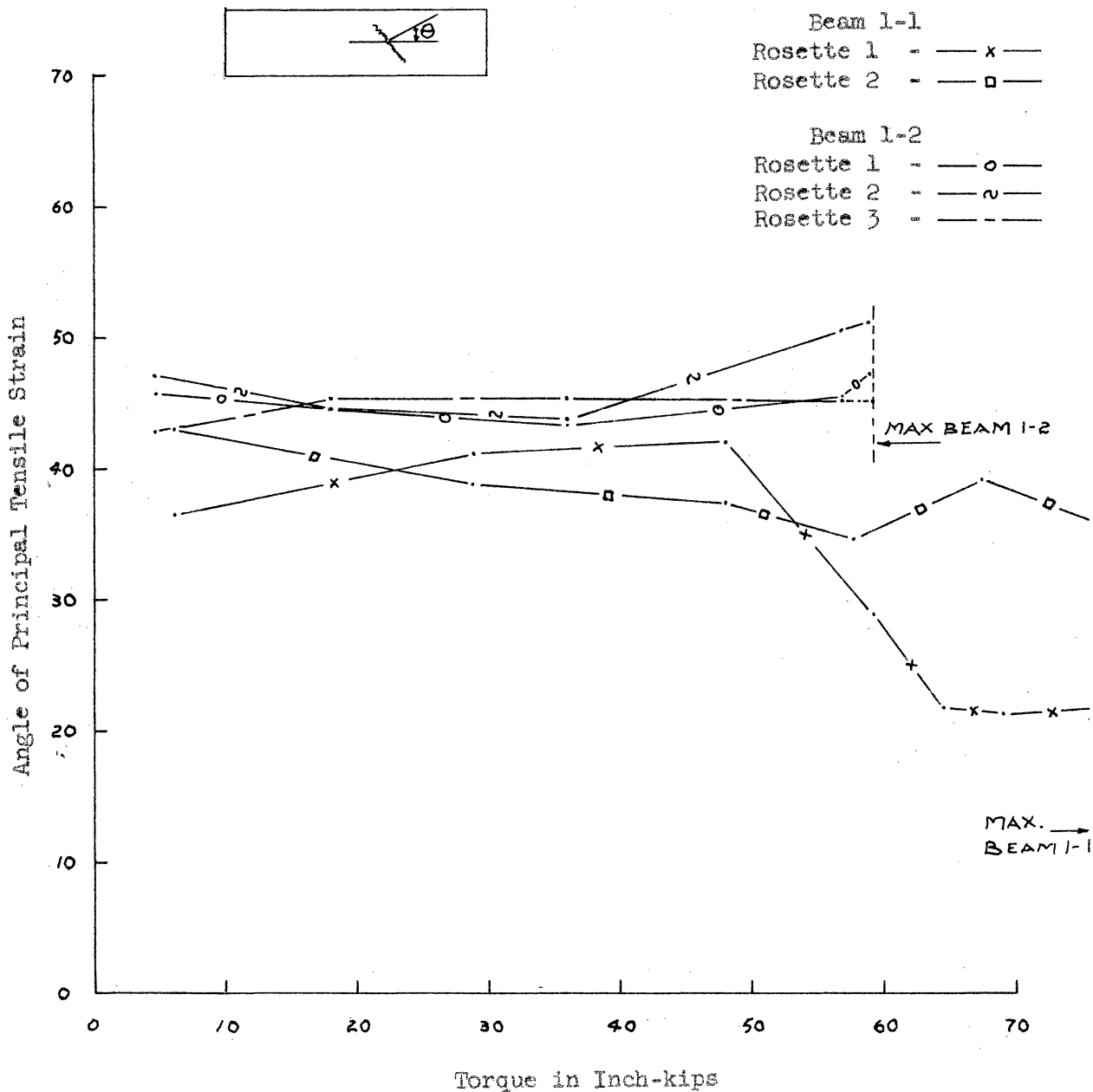


Figure 3-25 Angle of Principal Tensile Strain versus Torque  
Beams 1-1 and 1-2

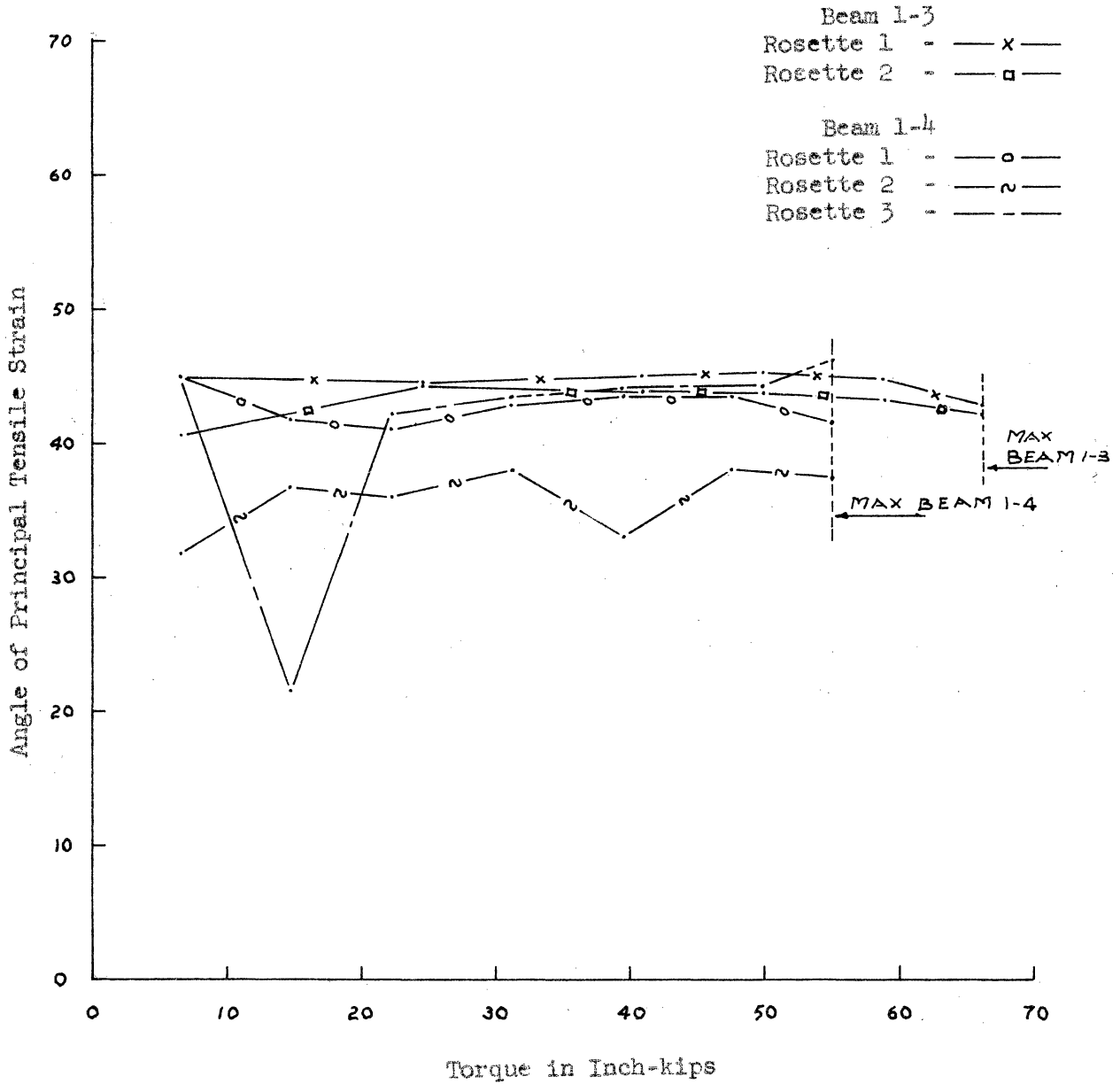


Figure 3-26 Angle of Principal Tensile Strain versus Torque  
 Beams 1-3 and 1-4

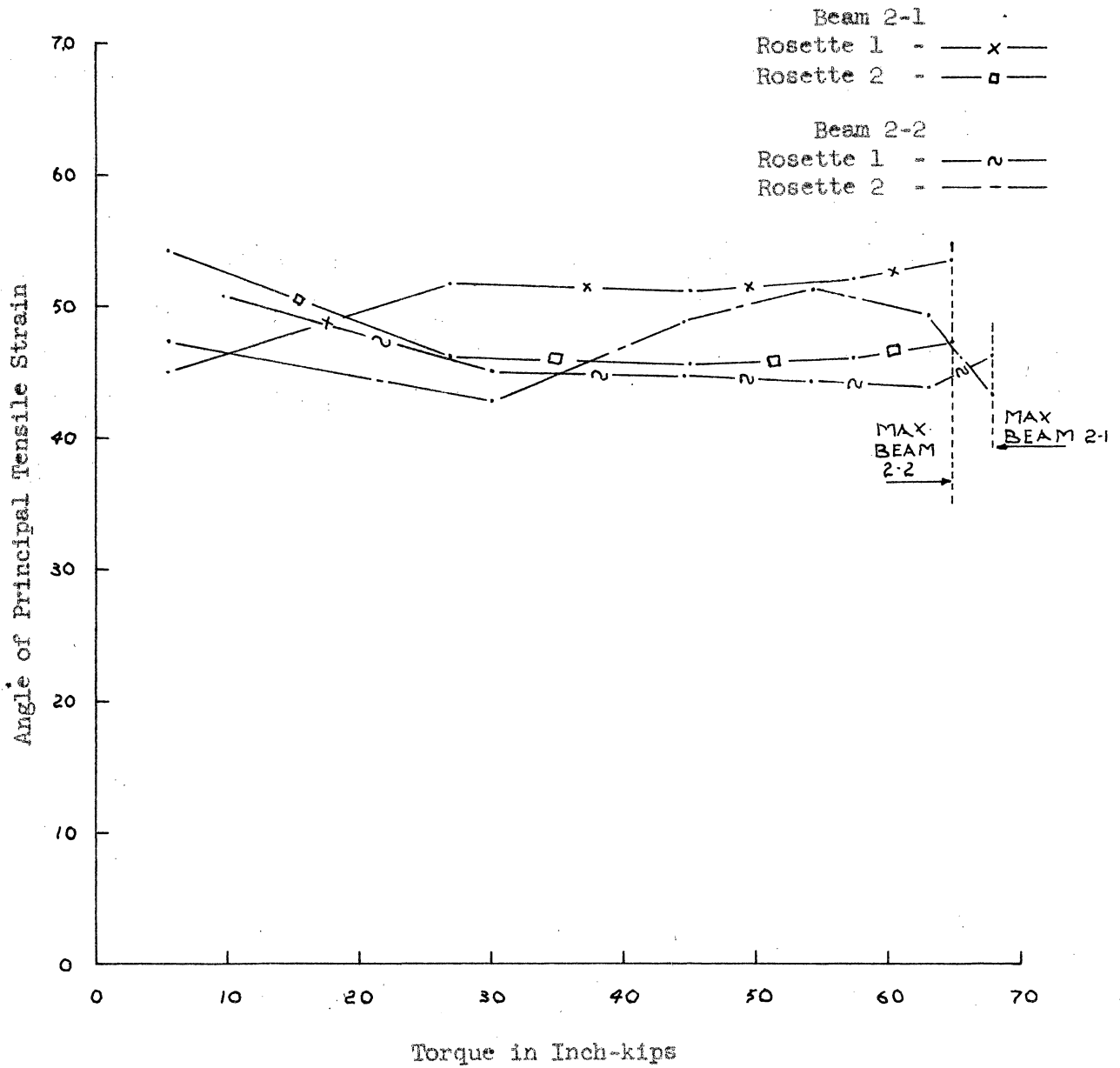


Figure 3-27 Angle of Principal Tensile Strain versus Torque  
Beams 2-1 and 2-2

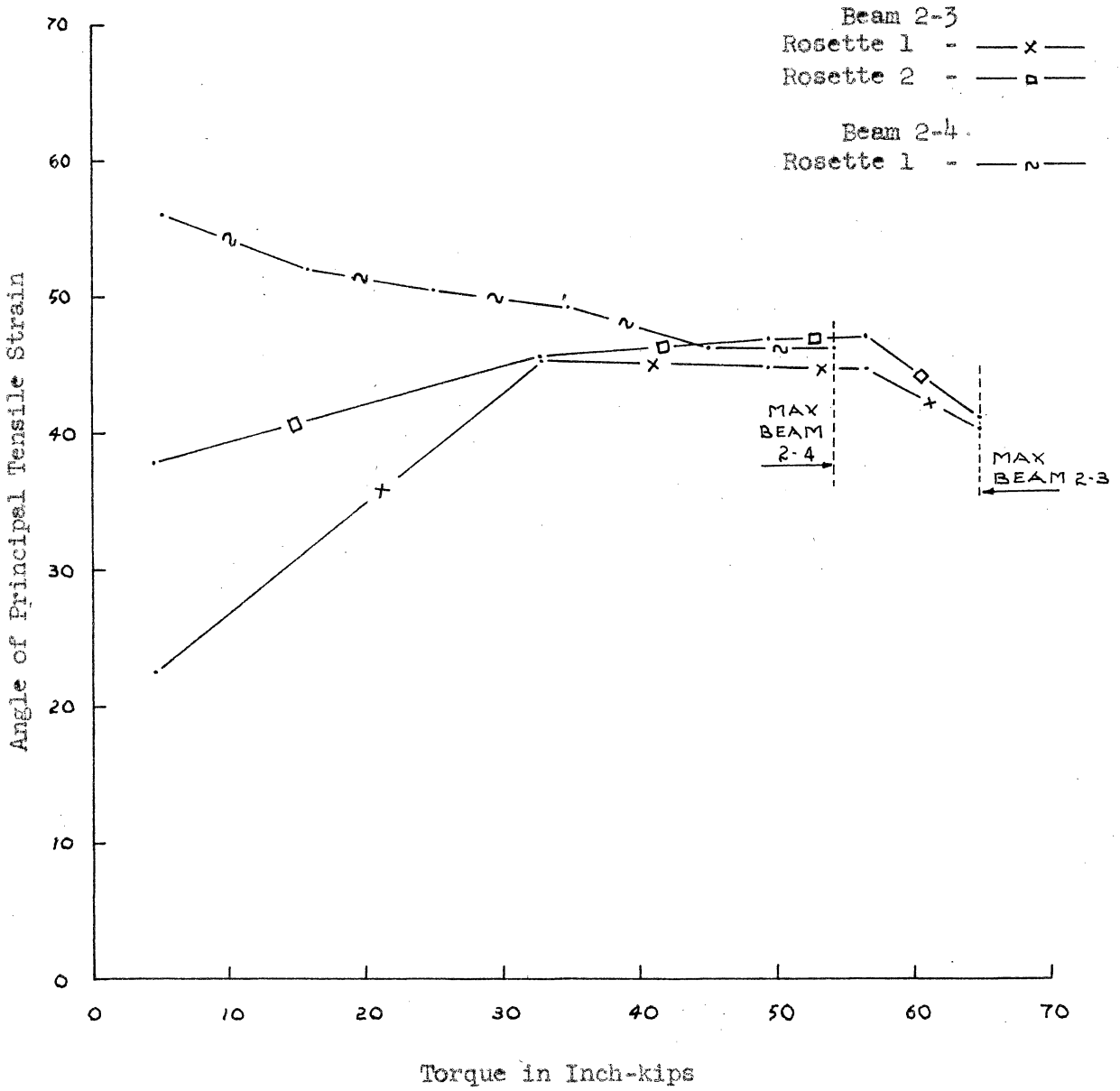


Figure 3-28 Angle of Principal Tensile Strain versus Torque  
Beams 2-3 and 2-4

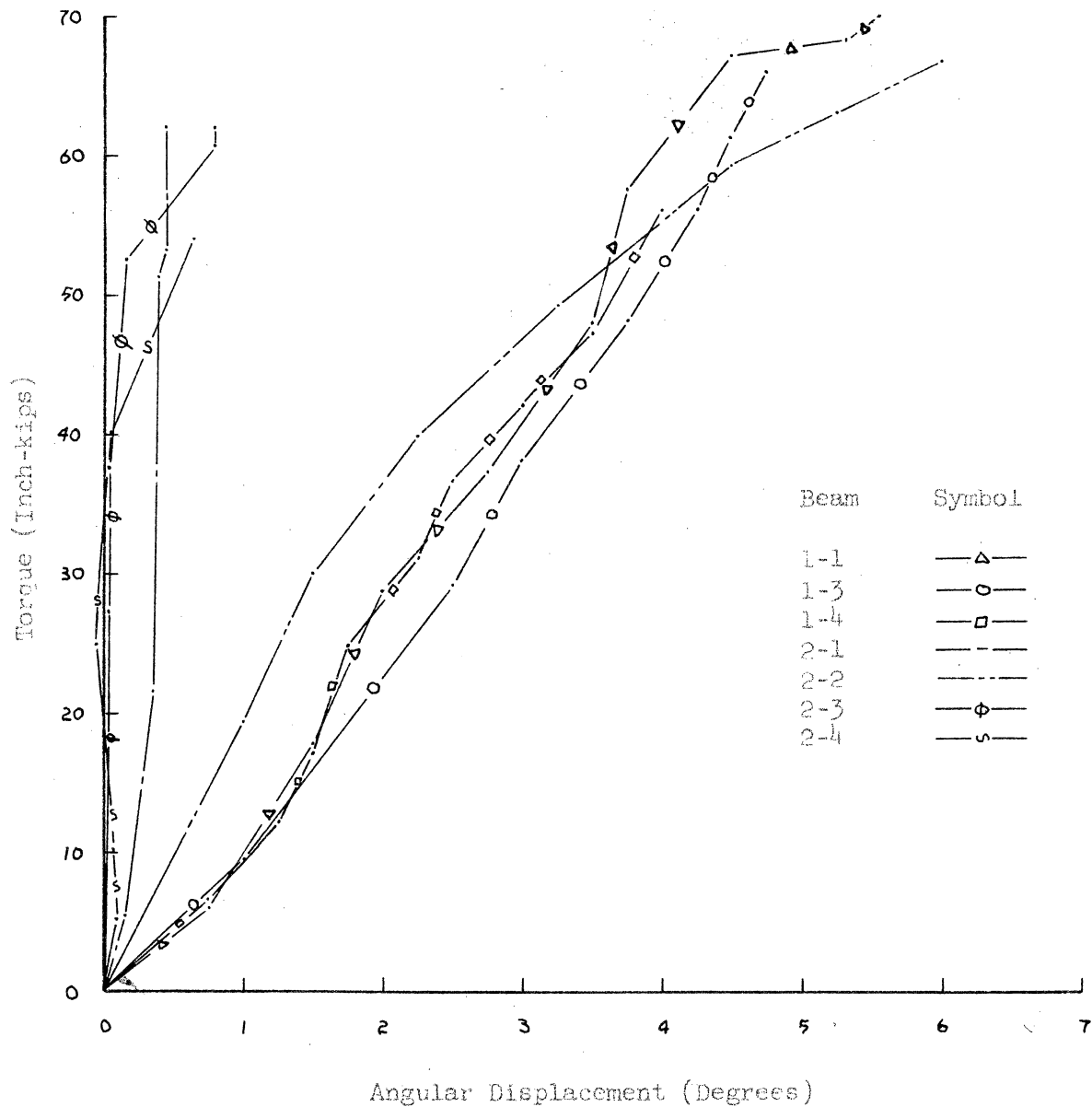
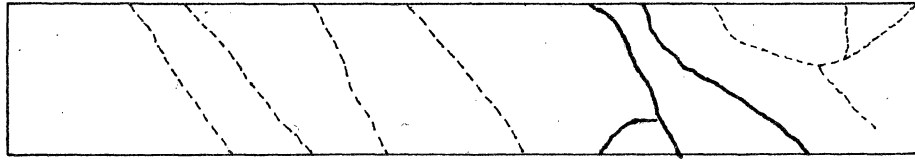
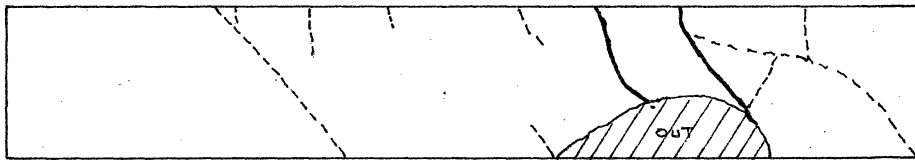


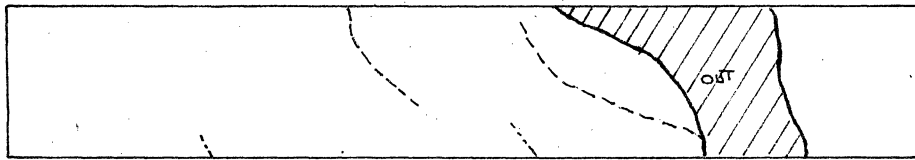
Figure 3-29 Angular Displacement versus Torque



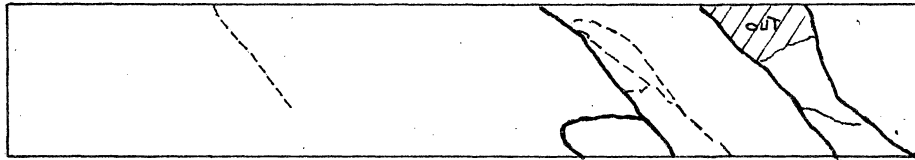
Top



Side

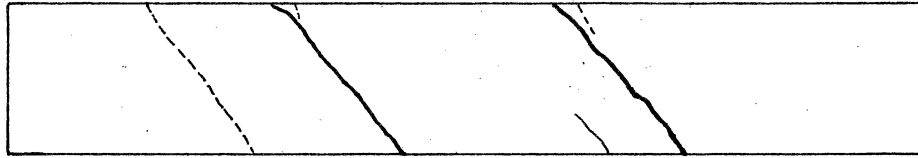


Bottom

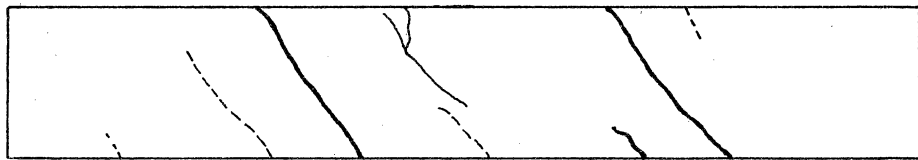


Side

Figure 3-30 Failure Cracks, Beam 1-1



Top



Side

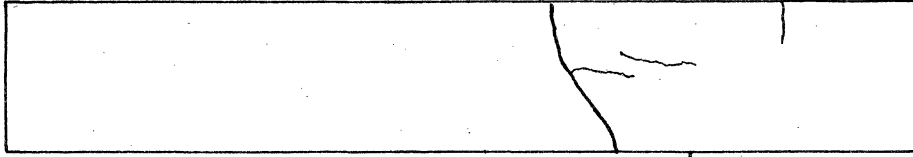


Bottom

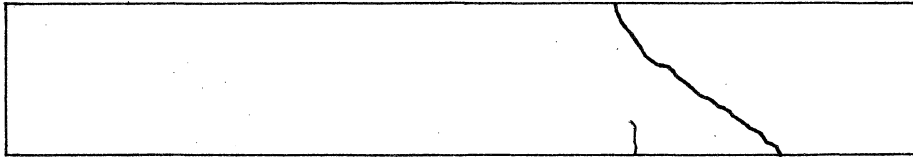


Side

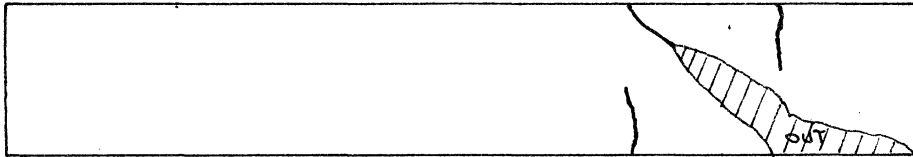
Figure 3-31 Failure Cracks, Beam 1-2



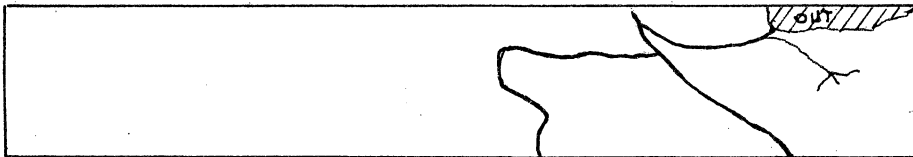
Top



Side

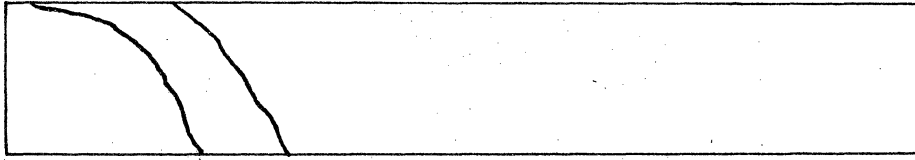


Bottom

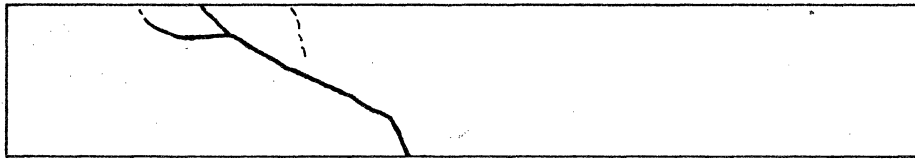


Side

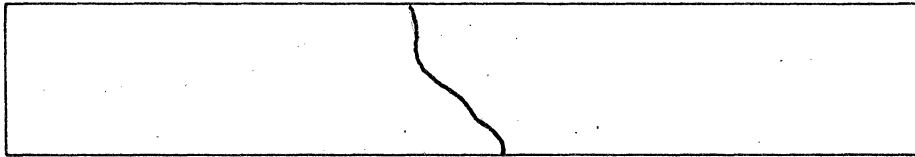
Figure 3-32 Failure Cracks, Beam 1-3



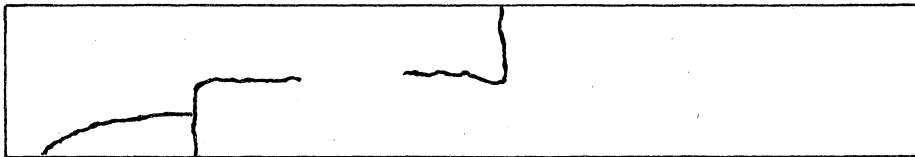
Top



Side

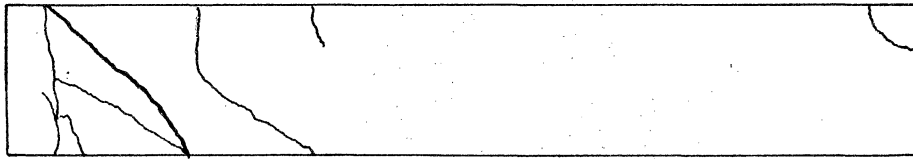


Bottom

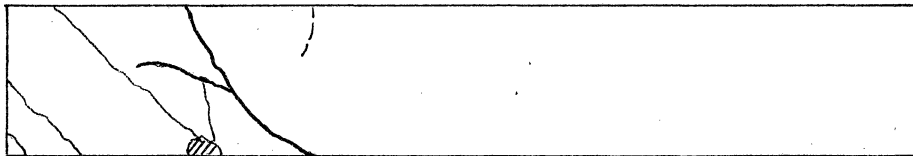


Side

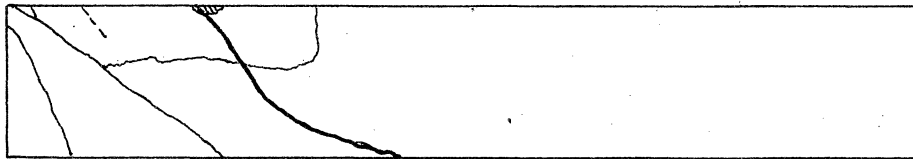
Figure 3-33 Failure Cracks, Beam 1-4



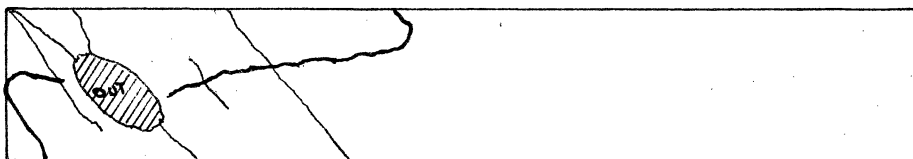
Top



Side

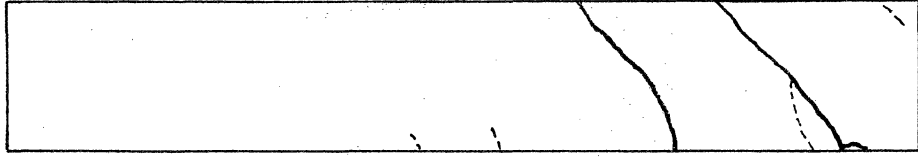


Bottom

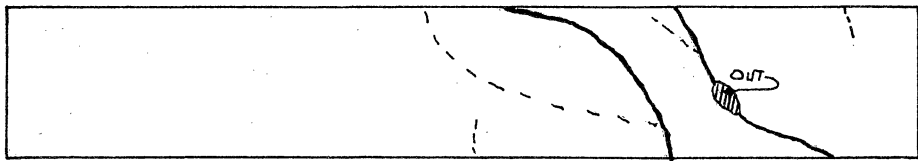


Side

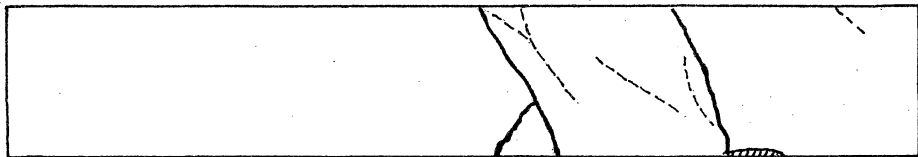
Figure 3-34 Failure Cracks, Beam 2-1



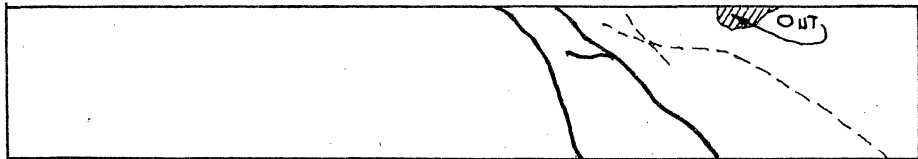
Top



Side

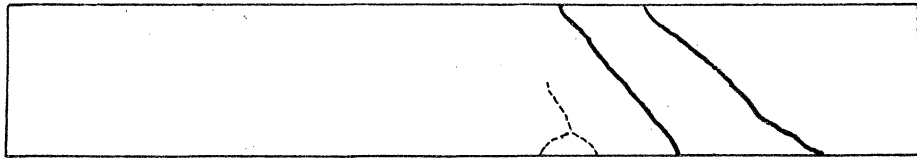


Bottom

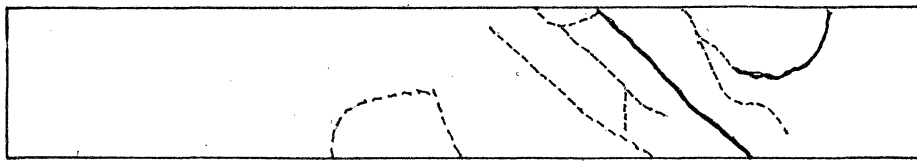


Side

Figure 3-35 Failure Cracks, Beam 2-2



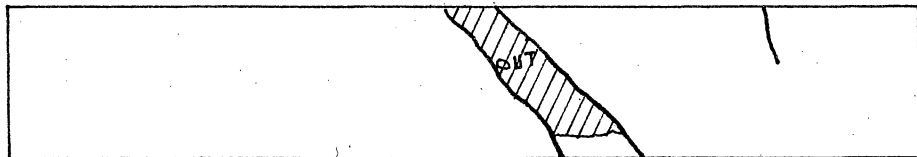
Top



Side



Bottom

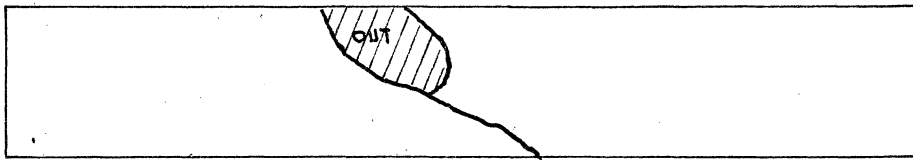


Side

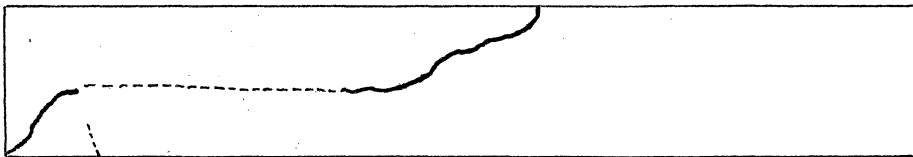
Figure 3-36 Failure Cracks, Beam 2-3



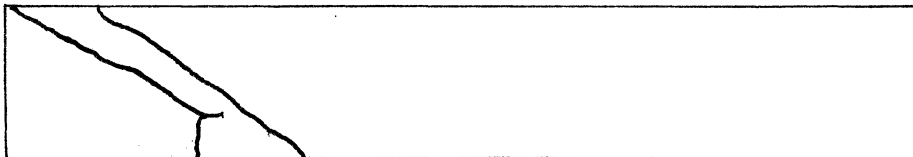
Top



Side



Bottom



Side

Figure 3-37 Failure Cracks, Beam 2-4

JUL • 63

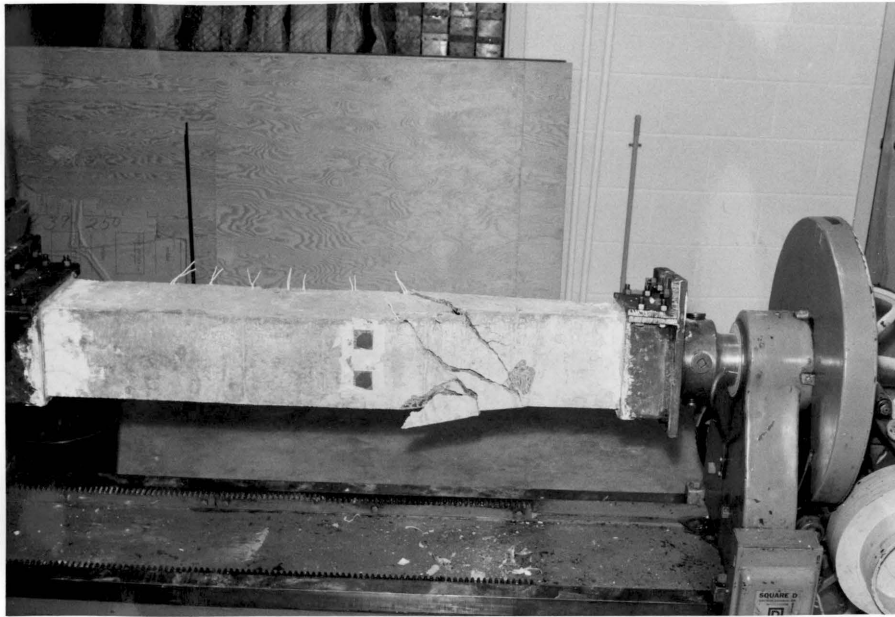


Figure 3-38 Failure Cracks, Beam 1-1

JUL • 63



Figure 3-39 Failure Cracks, Beam 1-1



AUG • 63

Figure 3-40 Failure Cracks, Beam 1-3



AUG • 63

Figure 3-41 Failure Cracks, Beam 1-4

AUG • 63



Figure 3-42 Failure Cracks, Beam 2-2

AUG • 63



Figure 3-43 Failure Cracks, Beam 2-2



Ε9 • 007

Figure 3-44 Failure Cracks, Beam 2-4

AUG • 63



Figure 3-45 Failure Cracks, Beam 2-4

#### IV. DISCUSSION

Although the primary objective of the program of which this thesis is a part is the practical analysis of a reinforced concrete beam subjected to combined bending and torsion, the purpose of this thesis was to review and extend, both experimentally and analytically, the investigation of the torsional resistance only. In previous theoretical and experimental work dealing with reinforced concrete beams in torsion two conflicting assumptions have been presented. One, that at the ultimate torque only the steel resists the tensile stresses, with both the steel and concrete resisting the compressive stresses; and two, that both the concrete, in a plastic state, and the steel resist both the tensile and compressive stresses induced. For this thesis eight beams were tested and the data evaluated to determine if there would be definite agreement with either assumption.

Seven of the eight beams tested failed suddenly with little or no warning. Only two (1-1, 2-1) of the seven beams showed evidence of cracking before the ultimate torque was reached. On these beams the cracks were hairline cracks, and although with increased torque the length of the cracks increased, the widths did not appear to increase until failure. At ultimate load and failure in the other five beams, the concrete seemed to crack along one failure zone instantaneously, leaving only the steel reinforcing to resist the applied torque. In no case was the steel able to resist any additional torque, nor to hold the maximum torque, and the beam failed.

The failure surface of each beam was outlined in general by a single predominating crack. These are shown by heavy lines on Figures 3-30 through 3-37. In one beam (2-1) the failure occurred close to one end where several parallel cracks opened up, and it was impossible to rank the various cracks as to their importance or to determine the failure surface conclusively. Failure occurred generally near the center in the other beams. The failure surface of five of the other seven beams was similar to that reported previously by Cowan<sup>(7)</sup>, Ernst<sup>(11)</sup> and Gesund<sup>(12)</sup> (Fig. 1-2), with a spiral tension crack around on three sides returning on itself through a compression hinge zone on the fourth side.

The failure surface of two beams (1-1, 2-2) differed. These two beams had greater ultimate torques than any of the other six, and failed with an explosive brittle type failure. The failure in both cases seemed to be a hybrid failure, with the concrete tending to fail in tension at an angle greater than  $45^\circ$ , rather than at  $45^\circ$  as experienced in unreinforced beams. This phenomenon is particularly noticeable in Beam 1-1, which is heavily reinforced (ties at 2" spacing), with its relatively short failure zone. Ernst<sup>(11)</sup> predicted a failure of this sort for heavily reinforced beams.

Beam 2-1 (ties at 2" spacing), which was theoretically stronger than Beam 2-2 (ties at 4" spacing) because of closer tie spacing, failed near one end at a lower ultimate torque. This was probably due to the lack of extra reinforcement near the end where the chuck induced local stresses which were probably very high. This was the only beam that did

not have extra ties at the ends to prevent failure at the chuck.

Although these tests were designed as pure torsion tests, there was some dead load bending moment present. At failure the moment/torque ratio was about 0.04. Apparently this had little if any effect; at least it did not induce the compression hinge to form on the top in each test. Four of the beams had a compressive hinge form on a side (1-3, 1-4, 2-1, 2-3) and two on the bottom (2-2, 2-4). There was no distinguishable compressive hinge on the other two beams (1-1, 1-2). In normally reinforced beams subjected to combined bending and torsion, the bending moment always causes the hinge to form on the top compression face of the beam<sup>(5)</sup>.

The steel strains in these beams remained small (up to 50-100 micro-inches per inch) until a relatively large torque caused the first crack to appear. In no case was there a general yielding of the reinforcement. On the contrary, there were only a few isolated cases where yield strains were recorded. Two longitudinal bars in Beam 1-3 showed yield strains at the ultimate torque. Both gages were near a predominant crack. It is very likely that some of the strains read from these two gages involved bending strains also. The other three cases where yield strains were recorded were in Beam 2-2, on one top longitudinal bar and on one stirrup, and in Beam 2-3, on one stirrup. The yield strains were not recorded until after the ultimate torque was reached and additional rotation was induced. These gages were in uncracked portions of the beam.

The only beam that did not exhibit a sudden type failure was

Beam 1-2, with ties at 4" spacing. This beam failed by a gradual yielding with new cracks forming continually throughout the test instead of the existing cracks widening. The initial cracks appeared early in the test with a small applied torque. The cracks did not appear to develop further when additional torque was applied. The concrete, although forty days old, seemed to crack readily (compared with the other beams), leaving only the steel to resist the tension. The predicted failure surface with the compressive hinge did not form in this beam. The spiral cracks formed, but none predominated to come back on itself and define a failure surface. After the ultimate torque was reached, the beam was still able to resist a reduced torque, although accompanied by severe creep. The action of this beam tends to justify the assumption mentioned previously that only the steel can be relied upon to resist the tensile stress at the ultimate torque.

The torque-strain relations (Fig. 3-13 through 3-24) in most cases seem reasonable and consistent with predictions. Notable exceptions are for Beam 2-1, where all the gages indicated compression up to a torque of about 35 inch-kips before straining in a tensile direction. No valid explanation can be found for this phenomenon except that the dummy gage or the battery-operated strain indicator developed a slow gradual drift during the test. Gage 2 in Beam 2-2 also showed compressive strains inconsistent with predictions, but this could very well have been due to localized effects from the end chuck holding the beam near the gage. Other gages that show compression are limited to strains up to about 10 micro-inches per inch, which are

within the range of experimental errors and indicate only that the strains are very small.

Rosette 3 on Beam 1-4 showed a tendency for the principal strain to indicate increased longitudinal tension at a torque of about 15 inch-kips. This could have been due to a false start of a compression hinge on the opposite face.

As a means of comparison, Table 2 was prepared giving the theoretical ultimate torques computed by methods suggested by three investigators, and the test value ultimate and cracking torque. In Ernst's ultimate strength formula the factor  $(k_v + k_n)$  was taken at 2.0, as suggested in Chapter II. Ernst's equation for the beams with no ties is the same as the elastic equation suggested by Cowan, but Ernst uses the ultimate tensile strength of the concrete instead of the allowable elastic strength. The part of Cowan's ultimate torque formula predicting the torque carried by the reinforcing steel alone is also given (Equation 2).

The estimated cracking torque for the test beams was obtained by assuming that the concrete cracked when the principal tensile strains reached a value of approximately 100 micro-inches per inch. The cracking torque reported was the smallest torque at which any of the principal tensile strains reached a value of 100 micro-inches per inch in tension.

It was expected that the maximum strain would occur on the centerlines. An evaluation of the strain data showed a random distribution for the location of maximum strain on those beams where

TABLE 1

Comparison of Various Theoretical Predictions with Test Results

(All Values in Inch-kips)

SPAN (Stirrup Spacing)	PREDICTIONS					TEST RESULTS	
	COWAN'S ELASTIC FORMULA*	COWAN'S ULTIMATE ST. FORMULA**	COWAN'S ULTIMATE FORMULA**	ERNST'S ULTIMATE FORMULA**	GESUND'S ULTIMATE FORMULA**	ESTIMATED CRACKING TORQUE	ULTIMATE TORQUE
	Eq.(1)+(2)	Eq.(2)	Eq.(2)+(3)	Eq.(5)	Eq.(11)		
1-1 (2")	72.0	82.5	168.6	65.0 <sup>†</sup>	210.1	54.4	76.0
1-2 (4")	57.2	41.2	127.3	66.0 <sup>†</sup>	105.0	55.0	58.9
1-3 (6")	52.2	27.5	113.6	66.0	70.0	49.9	66.0
1-4 (No ties)	9.3	----	86.1	53.7	----	47.6	55.0
2-1 (2")	68.6	82.5	155.1	66.0 <sup>†</sup>	210.1	57.5	64.7
2-2 (4")	53.8	41.2	113.8	66.0 <sup>†</sup>	105.0	44.6	67.7
2-3 (6")	48.8	27.5	100.1	66.0	70.0	49.4	61.8
2-4 (No ties)	8.6	----	72.6	45.4	----	50.4	54.1

\*Using 1963 ACI Building Code Values

With stirrups:  $f_{max} = 5 \sqrt{f'_c}$ ;  $f_s = 18,000$  psi;  $f'_c$  group 1 = 6301 psi;

$f'_c$  group 2 = 5320 psi

Without stirrups:  $f_{max} = 1.1 \sqrt{f'_c}$

\*\* $t_{ult} = .08 f'_c$ ;  $f_s$  yield = 50,000 psi;  $k_v + k_n = 2.0$

†Basic equation modified for less than minimum longitudinal steel. See text, p. 78.

rosettes were placed both on and off the centerlines. On those beams where rosettes were not on the centerlines, the cracking torque was computed for the 100 micro-inch per inch strains on the gages off the centerlines.

An examination of Table 2 shows several interesting things:

- 1) There is quite a wide range in the predicted ultimate capacities for every beam.
- 2) Most predicted ultimate capacities are greater than the actual test values, which means that the prediction equations would have been dangerous to use for the design of these beams.
- 3) Except for the beams with no ties (1-4, 2-4), Cowan's working capacities do not provide an adequate safety factor against the test failure values of these beams.
- 4) The use of ties increased the ultimate capacity of the test beams about twenty per cent.
- 5) The ultimate capacities of the test beams exceeded the cracking capacities by a wide range, from seven per cent to fifty-one per cent.
- 6) Cowan's ultimate capacity for the reinforcing steel alone gives a reasonable prediction for the test beams, if it is assumed that the contribution of the concrete is less as the quantity of the ties is increased.

The four longitudinal bars used meet the minimum requirements of Ernst's Equation (4) only in those beams (1-3, 2-3) with the stirrups spaced at six inches. According to Ernst, in test beams 1-1, 1-2, 2-1

and 2-2 the longitudinal steel would have yielded, causing the beams to fail before the closer spaced stirrups could develop yield stresses. If the area of longitudinal reinforcement is less than that required by Equation 4, the torque capacity can be computed by assuming that the maximum force that can be developed in the stirrups is proportional (Equation 4) to the area of the longitudinal reinforcement provided. Therefore Beams 1-1, 1-2, 2-1 and 2-2 would carry the same ultimate torque of 66.0 inch-kips.

Only Beam 2-2 had yield strains recorded in the longitudinal steel, although there could have been local yielding that was not picked up by the gages. Beam 1-1, with less than the minimum longitudinal steel for stirrups spaced at two inches, had a substantially higher ultimate torque than any other beam tested, which would support Gesund's or Cowan's predictions rather than Ernst's.

A further study of the test data shows that the presence of stirrups increases the torque capacity, but that the concrete is also effective in resisting the torque at ultimate conditions, since the beams with higher strength concrete failed generally at higher torque capacities. This action of the concrete was particularly evident in the beams that failed suddenly and did not develop visible cracks until the ultimate torque was reached.

The theories presented in Chapter II concerning reinforced concrete beams subjected to torsion assume an ideal failure surface of  $45^\circ$  cracks on three faces and a compressive hinge on the fourth face. This is based on the fact that the  $45^\circ$  plane is the principal plane

and experiences the greatest tensile force of any plane in the beam, regardless of whether the beam is of plain or reinforced concrete. If the beam is of plain concrete or reinforced in the longitudinal direction only, the  $45^\circ$  plane will probably be the failure plane, and equations based on this failure concept would be valid. But if the beam is reinforced with stirrups, the equations may not be entirely correct. With closely spaced stirrups the weakest plane will tend to be at an angle greater than the  $45^\circ$  plane. This angle increase allows the failure crack to cross fewer stirrups, while the diagonal tension that the stirrups are required to resist remains almost the same.

## V. CONCLUSIONS

In general the crack patterns and failure surfaces that occurred in these tests were similar to those previously reported by Cowan<sup>(7)</sup>, Ernst<sup>(11)</sup>, Gesund<sup>(12)</sup> and Sham<sup>(19)</sup>. Five of the beams had a failure surface similar to that shown in Figure 1-2. The two beams (1-1, 2-1) with the stirrups spaced at 2" had a hybrid shear-tension type of failure as predicted by Ernst<sup>(11)</sup>. The eighth beam (1-2), with stirrups spaced at 4", as well as Beam 1-1, had a unique crack pattern in that apparently no compressive hinge formed. After the ultimate torque was reached in Beam 1-2, additional torque was applied in hopes of forcing a noticeable hinge to form, but the beam developed new cracks in the spiral pattern instead. This beam was the youngest beam tested (forty days as compared to the others at about fifty-six days), and the concrete seemed to crack easily and uniformly, transferring the applied torque to the steel. The other seven beams, as described in Chapter IV, failed suddenly, and in some cases did not develop visible cracks until the ultimate torque was reached.

A comparison of theoretical predictions with the test results (Table 2) indicates that apparently no single formula is valid for all the test beams; however, Ernst's equation as limited by the longitudinal steel area is reasonably accurate. Cowan's elastic equations yield results that are too close to the ultimate torques for the members to be considered safe. This substantiates a similar conclusion previously reached by Sham<sup>(19)</sup>. However, this is only true of

those beams that contained stirrups. The beams that had no stirrups had an ultimate torque about five times Cowan's predicted elastic torque, which would indicate that either the allowable stress used was too conservative, or that Cowan's equation may not be valid, or that he did not give credit to dowel action of the longitudinal steel.

Gesund's ultimate torque equation was relatively accurate in predicting the capacity for the beams with stirrups spaced at 6". But the beams with stirrups at 2" and 4" had an ultimate torque calculated from both Cowan's and Gesund's equations much greater than the test ultimate torque. This may be explained by the hybrid shear-tension type failure observed in Beams 1-1 and 2-2 instead of a tensile type failure on which the equations are based.

There was no significant information gained as to the bending moment induced in a beam by the action of stresses in the stirrups. It was hoped that the bending moment could be measured by measuring the strains in the longitudinal steel, but the differences between longitudinal strains on opposite faces of the beams were too inconsistent to develop a usable equation. In none of the tests of beams with stirrups did the crack pattern develop over the area where the strain gages were placed so that useful data could be obtained.

## BIBLIOGRAPHY

1. Andersen, Paul. "Experiments with Concrete in Torsion," Transactions of the American Society of Civil Engineers, Volume 100, 1935, pp. 949-983.
2. Andersen, Paul. "Rectangular Concrete Sections Under Torsion," Proceedings of the American Concrete Institute, Volume 34, 1938, pp. 1-11.
3. Hoaz, I. B. "Combined Bending and Torsion in Reinforced Concrete Beams." Thesis for the degree of Master of Science, Virginia Polytechnic Institute, 1962.
4. Bresler, Boris. "Discussion of a Paper by Henry J. Cowan," Proceedings of the American Concrete Institute, Volume 56, 1959-1960, pp. 1389-1400.
5. Buchanan, G. R. "Ultimate Strength of Rectangular Concrete Beams with and without Transverse Reinforcing in Combined Bending and Torsion." Thesis for the degree of Master of Science, University of Kentucky, 1962.
6. Cowan, H. J. "Design of Beams Subject to Torsion Related to the New Australian Code," Proceedings of the American Concrete Institute, Volume 56, 1959-1960, pp. 591-618.
7. Cowan, H. J. "An Elastic Theory for the Torsional Strength of Rectangular Reinforced Concrete Beams," Magazine of Concrete Research, Volume 2, Number 4, July, 1950, pp. 3-8.
8. Cowan, H. J. "The Strength of Plain, Reinforced and Prestressed Concrete Under the Action of Combined Stresses, with Particular Reference to Combined Bending and Torsion of Rectangular Sections," Magazine of Concrete Research, Volume 5, Number 14, December, 1953, pp. 75-86.
9. Cowan, H. J. "Torsion of a Rectangular Elastic Isotropic Beam Reinforced with Rectangular Helices of Another Material," Applied Scientific Research, Volume 3, 1951-1953, pp. 344-348.
10. Cowan, H. J. and Armstrong, S. "Experiments on the Strength of Reinforced and Prestressed Concrete Beams and of Concrete-Encased Steel Joists in Combined Bending and Torsion," Magazine of Concrete Research, Volume 6, Number 19, March, 1955, pp. 3-20.

11. Ernst, G. C. "Ultimate Torsional Properties of Rectangular Reinforced Concrete Beams," Proceedings of the American Concrete Institute, Volume 54, 1957-1958, pp. 341-356.
12. Gesund, Hans. "Ultimate Strength of Reinforced Concrete Beams in Combined Torsion, Bending and Shear." Unpublished paper of Professor Gesund, University of Kentucky, 1960.
13. Grassan, N. S. J. "Experiments on Concrete Under Combined Bending and Torsion," Proceedings of the Institution of Civil Engineers, Volume 5, Number 2, March, 1956, pp. 159-165.
14. Lessig, N. N. "Determination of the Load-Bearing Capacity of Reinforced Concrete Elements with Rectangular Cross Section Subjected to Flexure with Torsion," Proceedings, Concrete and Reinforced Concrete Institute, Volume 5, Moscow, 1959. (Translated from Russian by Margaret Corbin, Foreign Literature Study Number 371.)
15. Marshall, W. T. "The Torsional Resistance of Plastic Materials with Special Reference to Concrete," Concrete and Constructional Engineering, Volume 39, Number 4, 1944, pp. 83-88.
16. Nadai, Arpad. Theory of Flow and Fracture of Solids, Volume 1, Second Edition, McGraw-Hill Book Company, 1950, pp. 490-511.
17. Pandit, G. S. "Ultimate Strength of Reinforced Concrete in Torsion," Cement and Concrete, July-September, 1962.
18. Schuette, F. J. "Ultimate Strength of Square Concrete Beams with Transverse Reinforcing in Combined Bending and Torsion." Thesis for the degree of Master of Science, University of Kentucky, 1962.
19. Sham, E. Q. "Ultimate Strength Theory of Torsion Applied to Reinforced Concrete Beams." Thesis for the degree of Master of Science, University of Kentucky, 1960.
20. Timoshenko, Stephen. Strength of Materials, Part II, Third Edition, D. Van Nostrand Company, 1956, pp. 237-254.
21. Young, C. R., Sager, W. L. and Hughes, C. A. "Torsional Strength of Rectangular Sections of Concrete, Plain and Reinforced," The American Architect and the Architectural Review, Volume 124, Number 2425, August 1, 1923, pp. 121-126.

**The vita has been removed from  
the scanned document**

# ANALYSIS OF A REINFORCED CONCRETE BEAM IN TORSION

by

William Aurand Stuart II

## ABSTRACT

Eight reinforced concrete beams with two different concrete strengths and four different schemes of reinforcing were tested to failure in pure torsion. SR-4 strain gages were used to measure the steel strains at selected points, while strain rosettes were used to measure the concrete strains at the surface of the test beams.

A review of analytical and experimental studies in the literature is presented and briefly discussed. The test results were then compared with the theoretical predictions developed by Cowan, Ernst and Gesund.

In general the failure surface of the test beams agreed with those previously predicted. The test ultimate torque varied considerably from the predicted ultimate torques of Cowan and Gesund. Ernst's basic equation was modified to compensate for less than the minimum longitudinal reinforcement in four of the beams. With this modification Ernst's theoretical predictions were very close to the test results.

A study of the test results also shows that one of the presented theories is valid for one particular case, but that none of the theories is valid for every case. Consequently, there is a need for further research in this subject in order to develop a more exact theory for use in design.